



## Arctic Ocean outflow and glacier-ocean interaction modify water over the Wandel Sea shelf, northeast Greenland

Igor A. Dmitrenko<sup>1\*</sup>, Sergei A. Kirillov<sup>1</sup>, Bert Rudels<sup>2</sup>, David G. Babb<sup>1</sup>, Leif Toudal Pedersen<sup>3</sup>, Søren  
5 Rysgaard<sup>1,4,5</sup>, Yngve Kristoffersen<sup>6,7</sup> and David G. Barber<sup>1</sup>

<sup>1</sup>Centre for Earth Observation Science, University of Manitoba, Winnipeg, Canada

<sup>2</sup>Finnish Meteorological Institute, Helsinki, Finland

<sup>3</sup>Danish Meteorological Institute, Copenhagen, Denmark

10 <sup>4</sup>Greenland Climate Research Centre, Greenland Institute of Natural Resources, Nuuk, Greenland

<sup>5</sup>Arctic Research Centre, Aarhus University, Aarhus, Denmark

<sup>6</sup>Department of Earth Science, University of Bergen, Bergen, Norway

<sup>7</sup>Nansen Environmental and Remote Sensing Centre, Bergen, Norway

15 \*Corresponding author, e-mail: [igor.dmitrenko@umanitoba.ca](mailto:igor.dmitrenko@umanitoba.ca)

**Abstract:** The first-ever conductivity-temperature-depth (CTD) observations on the Wandel Sea shelf in North Eastern Greenland were collected in April-May 2015. They were complemented by CTD profiles taken along the continental slope during the Norwegian FRAM 2014-15 drift. The CTD profiles



20 are used to reveal the origin of water masses and interactions with ambient water from the continental  
slope and the outlet glaciers. The subsurface water is associated with the Pacific Water outflow from the  
Arctic Ocean. The underlying Halocline separates the Pacific Water from a deeper layer of Polar Water  
that has interacted with the warm Atlantic water outflow through Fram Strait recorded below 140 m.  
Over the outer shelf, the Halocline shows numerous cold density-compensated intrusions indicating  
25 lateral interaction with an ambient Polar Water mass across the continental slope. At the glacier front,  
colder and turbid water intrusions were observed at the base of the Halocline. In temperature-salinity  
space, these data follow a mixing line that diverges from ambient water properties and indicates ocean-  
glacier interaction. Our observations of Pacific Water are set within the context of upstream  
observations in the Beaufort Sea and downstream observations from the Northeast Water Polynya and  
30 clearly show the modification of Pacific water during its advection across the Arctic Ocean. Moreover,  
ambient water over the Wandel Sea slope shows different thermohaline structures indicating the  
different origin and pathways of the on-shore and off-shore branches of the Arctic Ocean outflow  
through western Fram Strait.

## 35 **1. Introduction**

One of the most significant global issues over the last decade has been the vast change in the  
Arctic region. The Arctic Science Partnership (ASP) consortium ([www.asp-net.org](http://www.asp-net.org)) was established to  
understand connections and processes linking climate, cryosphere, ocean and ecosystems. Under the  
framework of ASP, an extensive oceanographic field campaign took place during April and May 2015  
40 from the landfast sea ice that covers the shelf of the Wandel Sea.



The field campaign was based out of the new Villum Research Station located at the Danish military outpost Station Nord at 81°36N, 16°40W on Prinsesse Ingeborg Peninsula in the very north-eastern corner of Greenland (Figures 1 and 2). Northern Greenland is among the most remote wildernesses of the northern hemisphere. Station Nord features a very cold polar tundra climate with an average temperature during winter below -30°C and just a few degrees above the freezing point in the midst of the short summer. The Flade Isblink Ice Cap is located close to Station Nord (Figure 2b). It is an isolated ice cap with a surface area of 5 000 km<sup>2</sup> and maximum thickness of 600 m that overlies bedrock that is on average 100 m below sea level [e.g., *Palmer et al.*, 2010; *Rinne et al.*, 2011].

Prior to our field program in 2015, there were no oceanographic or *in situ* sea ice observations over the Wandel Sea shelf. *Nørgaard-Pedersen et al.* [2008] provided limited information on the bottom topography in the area, specifically the existence of several submarine glacial troughs, with depths of up to ~180 m, that open to the continental slope (Figure 3). From very general considerations, the Wandel Sea shelf is expected to be under the influence of the Arctic Ocean outflow through western Fram Strait (Figure 1). The upper layer (down to 400 m) of this outflow is comprised of low salinity surface Polar Water which is partially composed of Pacific-origin water, and the intermediate water (> 150-200 m) of Atlantic origin [e.g., *Rudels et al.*, 2002; 2005]. The freshwater export through western Fram Strait is an important component of the Arctic Ocean freshwater budget that links the Arctic Ocean to the global climate system [e.g., *de Steur et al.*, 2009]. The Atlantic Water outflow through Western Fram Strait closes the circulation loop of the Atlantic Water in the Arctic Ocean conditioned by its inflow through eastern Fram Strait and Barents Sea [e.g., *Rudels et al.*, 1994; *Rudels*, 2012] –



Figure 1. The Wandel Sea shelf can also be a source of freshwater that originates from summer snow/sea ice meltwater and from glacier-derived freshwater.

This paper is focused on analysis of the first-ever conductivity-temperature-depth (CTD) observations on the Wandel Sea shelf collected from the landfast ice in April-May 2015. They were  
65 complemented by CTD profiles taken in June-July 2015 over the Wandel Sea continental slope during the Norwegian FRAM 2014-15 sea ice drift. Our objectives were to investigate the principal features of vertical profiles of salinity and temperature taken over the shelf regions deeper than 100 m.

The paper is structured as follows. Section 2 describes CTD casts, sea-ice and bottom topography, and justifies the selection of CTD data for our analysis. Section 3 provides detailed  
70 description of the water mass structure over the Wandel Sea shelf and continental slope, methods of clustering the CTD profiles, and the CTD clusters. Section 4.1 discusses oceanographic patterns of the “glacier” CTD cluster with respect to the ocean-glacier interaction. Section 4.2 focuses on the “intrusive” CTD cluster from the Wandel Sea outer shelf. Sections 4.3/4.4 discuss local/remote origins of the Wandel Sea water masses. Finally, section 5 concludes the analysis and discusses limitations.

75

## 2. Data and methods

Between 17 April and 15 May 2015, 86 CTD profiles (labelled SN15 – XX; XX is the station number) were collected from the landfast sea ice (1.0 to 3.5 m thick) on the Wandel Sea shelf in Northeast Greenland (Figure 3). The CTD observations were carried out with a SBE-19plus CTD that  
80 was calibrated prior to the expedition, and was accurate to  $\pm 0.005^{\circ}\text{C}$  and  $\pm 0.0005$  S/m. The CTD was outfitted with a Seapoint Turbidity Meter that measured turbidity in nephelometric turbidity units



(NTU). Additionally we used vertical profiles of the colored dissolved organic matter (CDOM) from an Ice Tethered Profiler (ITP) by McLane Research Laboratory that was temporarily deployed at SN15-13 from 21 April to 11 May. The ITP collected a profile every 2 hours between 3 m and 101 m depth, and  
85 was equipped with a Wetlabs ECO sensor for measuring backscatter intensity, Chlorophyll fluorescence and CDOM fluorescence for EX/EM = 370/460 nm. CDOM data was recorded approximately every 1.5 m with sensitivity of 0.28 parts per billion (ppb). Other ITP data from this temporary deployment are not used within this paper.

Four sets of complementary CTD profiles are used to provide context for the water masses we  
90 observed over the Wandel Sea shelf. CTD profiles collected in the Beaufort Sea between 225°E and 226°E meridians between June and October from 2002 to 2011 by ArcticNet were averaged and reveal the mean summer water profile in the Beaufort Sea, which we consider the ‘upstream’ area. CTD profiles collected over the Wandel Sea continental slope during June and July 2015 from the research hovercraft SABVABAA during the Norwegian FRAM 2014/15 sea ice drift (Figure 2b) are used to  
95 represent the ambient water masses and compared against a CTD profile collected in August 2008 from the RV *Polarstern* [Kattner, 2009]. Furthermore we adopted a CTD profile taken in a rift in the 79 North Glacier in August 2009 – Figure 2a [Straneo *et al.*, 2012].

Ice conditions over the Wandel Sea shelf, the adjoining fjords and the Greenland Sea continental slope were monitored by MODIS (Moderate Resolution Imaging Spectroradiometer – Figure 2) and  
100 Sentinel-1 C-band SAR (C-Band Synthetic Aperture Radar – Figure 3) satellite imagery, acquired daily by the Danish Meteorological Institute (<http://ocean.dmi.dk/arctic/nord.uk.php>). In general, newly



formed sea-ice, ice ridges, multiyear and first-year landfast sea ice, refrozen leads, large icebergs and glacier terminations are distinguishable in SAR imagery. Sea ice thickness was measured manually at each CTD station with an ice thickness tape.

105            Within this study we are interested in resolving the vertical thermohaline structure below the freshened surface waters, including the water layer below the lower boundary of the glacier tongue (>~90 m depth) and a warmer Atlantic-derived water layer with temperature > 0°C below ~140 m depth. Therefore we only use the 31 CTD profiles that were performed in waters deeper than 100 m (Figure 3).

110

### 3. Results

Over the Wandel Sea shelf there are three regions with depths greater than 100 m. These regions are separated laterally by ~20-30 m deep shoals, but are likely connected to submarine troughs that lead towards the continental slope [Nørgaard-Pedersen *et al.*, 2008].

115            Region 1 is located over a submarine glacial trough on the outer shelf that ranges in depth from 110-130 m at the tidewater glacier outlet (STN15-13 and 75) to 183 m further off-shore along the trough (STN15-63; Figure 3). The glacial trough has been formed by the Flade Isblink Ice Cap [e.g., Palmer *et al.*, 2010; Rinne *et al.*, 2011]. During our surveys this area was predominantly covered by landfast multiyear sea ice (~3.5 m thick; lighter colours in Figure 3). Several CTD stations were  
120 performed through refrozen leads that contained younger and therefore thinner sea ice (~1.5 m thick; darker colours in Figure 3). Region 1 was paralleled on both sides by numerous icebergs that appeared to be grounded on the marginal lateral moraine which can significantly suppress lateral exchange with



ambient water from the continental slope. However, lateral exchange still might be possible given the narrow glacial troughs that exist across these shallow shoals [Nørgaard-Pedersen *et al.*, 2008].

125           Region 2 is located over the mid shelf to the north of Station Nord between Prinsesse Thyra and Prinsesse Margreth Islands with depths of 104/112 m (stations STN15-53/54; Figure 3). The region was covered by ~1.2 m of sea ice that grew within a refrozen lead after it opened in August 2012 (Figure 3). We speculate that the gradual increase in depth along the CTD transect that ended at STN15-54 continues out along the trough towards the continental slope; however, no bathymetric data is available  
130 beyond STN15-54.

          Region 3 is located to the west-southwest of Station Nord along another glacial trough on the inner shelf that extends from the outlet glacier of the Flade Isblink ice cap to the west of Prinsesse Dagmar Island (Figure 3). During our field work the glacier was grounded at ~35-40 m depth. The trough extending from this outlet glacier quickly reached depths of ~100 m (STN15-35) and reached a  
135 maximum depth of 127 m (STN15-79). During the field campaign this region was covered with a mix of first year (~1.2 m thick) and multiyear sea ice (~3 m thick), with icebergs and an ice island frozen within the fast ice (Figure 3). Region 3 was ice-free during August 2014 (Figure 2) as well as during August 2010-2012 (<http://ocean.dmi.dk/arctic/nord.uk.php>).

          The water column over the Wandel Sea shelf deeper than 100 m shows six distinct layers  
140 (Figure 4). The layer immediately below the ice (~1.5–5 m) was relatively fresh (salinity of 16-21; Figure 4) as a result of summer snow/sea ice melt water and freshwater from the glacial runoff. Several stations had extremely fresh surface waters (salinity of 1-12; Figure 4) that appeared to be part of under-ice ponds [e.g. Eicken, 1994; Flocco *et al.*, 2015] comprised of melt water trapped in pockets below the



multiyear landfast ice. This surface layer freshened during the melt season and was observed to have  
145 salinities of 1-8 during CTD transects in August 2015 [Jørgen Bendtsen, pers. comm., 2016]. The sub-  
surface halocline layer is characterised by a strong vertical salinity gradient (salinity  $1 \text{ m}^{-1}$ ) down to 15  
m depth (Figure 4). The sub-surface halocline separated the fresh surface waters from a layer with weak  
vertical salinity gradients (salinity 30 to 31.2) and water near the freezing point (blue dashed line Figure  
4) that reached to  $\sim 65$  m depth (Figure 4). Shimada *et al.*, [2005] identified this layer in the Canada  
150 Basin and referred to it as a “cold halostad”, thus over the Wandel Sea shelf we refer to this layer as the  
“Halostad” (Figure 4, Table 1).

Below the Halostad (below 75 m depth), temperatures increased steadily through the Halocline  
(with salinity centered around 33) and Atlantic modified Polar Water (PrW) – Figure 4 and Table 1. The  
Halocline is further distinguished from the Halostad and PrW by its high vertical salinity gradient of  
155  $0.07 \text{ m}^{-1}$  (Figure 4). Temperatures eventually exceeded  $0^\circ\text{C}$  (the commonly accepted upper boundary of  
the Atlantic layer) at  $\sim 140$  m depth indicating the presence of Atlantic Water (AW) below this depth  
(Table 1). Atlantic modification of the Halocline is evident from the increase in temperature through the  
Halocline. Furthermore, the Halocline shows intrusions of cooler water, which is further described and  
discussed for tracing the shelf-slope and ocean-glacier interactions, as well as the Pacific Water (PcW)  
160 and AW outflow from the Arctic Ocean through western Fram Strait.

Comparing CTD profiles collected over the Wandel Sea shelf (solid lines) and those collected  
off-shelf (dashed lines) reveals substantial differences in the temperature profiles down to 180 m, and in  
the salinity profiles down to 110 m (Figure 4). In 2015, the Halostad and Halocline over the Wandel Sea





shelf were not observed over the continental slope (Figure 4). Moreover, the thermocline was typically  
165 20-30 m deeper off the shelf (red dashed lines Figure 4), specifically the upper boundary of the AW was  
found at 170 m compared to 140 m on the shelf. We also present a CTD profile collected on the upper  
continental slope in 2008 (dot lines in Figure 4), which reveal little variability in the water mass  
structure between 2008 and 2015 and indicate that the off-shelf water mass structure is characterized by  
a colder, thicker and more saline Halostad that is derived from the Lower Halocline in the Nansen Basin  
170 [Rudels *et al.*, 1996]. We note, however, that the synoptic, seasonal, and interannual variability can be  
significant [e.g., Falck *et al.*, 2005], making it difficult to interpret the snapshot data from the Wandel  
Sea continental slope.

In the following, we focus on the water layer below the sub-surface Halocline, comprised of the  
Halostad, Halocline, PrW and AW layers (Figures 4-6, Table 1). The 31 CTD profiles with depths  
175 greater than 100 m were subdivided into clusters according to their temperature-salinity ( $T$ - $S$ ) curves  
and their variability in  $T$ - $S$  space (Figures 5 and 6 and Table 2). For clustering we use the following  
criteria. (i) For the salinity range  $30 < S < 31.2$  (~15-65 m depth; Halostad; gray shaded area Figure 5)  
we differentiate profiles based on their proximity to the freezing temperature (blue dashed line Figure  
5), which indicates how the thermal properties of ambient waters have been modified. (ii) For the  
180 salinity range  $31.2 < S < 33.5$  (~65-90 m depth; upper Halocline; green shaded area Figures 5 and 6) we  
differentiate clusters based on the appearance of distinctive thermohaline intrusions within the TS  
curves. These intrusions increase the TS variability and disrupt the initially smooth TS curves, which  
indicate interaction between ambient water masses. These features have been used to trace the origin  
and pathways of water masses in the Arctic Ocean [e.g., Walsh and Carmack, 2003; Rudels *et al.*, 1994;



185 2005; Woodgate *et al.*, 2007] and identify shelf-glacier interactions [Jenkins, 1999; Stevens *et al.*,  
2015]. (iii) For the salinity range  $> 33.5$  ( $> 90$  m depth; low Halocline; pink shaded area; Figures 5 and  
6) we use the appearance of thermohaline intrusions and the slope of the mixing line to differentiate the  
clusters (Figure 6). The displacement of the mixing line indicates an external source of heat and/or salt  
is present and suggests a new mixing end member [e.g., Gade, 1979; Jenkins, 1999; Straneo *et al.*,  
190 2012; Wilson and Straneo, 2015].

The intrusions along isohalines suggest isopycnal interleaving (Figures 5b and 6). Thus, one  
along-isopycnal standard deviation of the mean temperature and salinity was employed to estimate the  
efficiency of intrusive activity for every  $0.1 \text{ kg m}^{-3}$  interval of the potential density. All TS curves  
exceeding  $\pm 1$  standard deviation at more than 50% of the  $0.1 \text{ kg m}^{-3}$  intervals were added to the  
195 different clusters based on the prescribed salinity range. We also defined a “transit” cluster (Figure 6a)  
showing weak thermohaline intrusions below one standard deviation of the mean.

Based on our criteria, all CTD profiles  $\geq 100$  m depth were subdivided into five clusters (Table  
2). Here we assess the main patterns of these clusters putting them in the context of their geographical  
location on the Wandel Sea shelf and the sea-ice features.

200 Cluster I is comprised of the nine CTD stations with depths greater than 100 m in Regions 2 and  
3 (SN15-31/35/53/54/79-83; Figure 7). This cluster is distinguished by two features: (i) a relatively  
warm Halostad overlying the Halocline above 65 m ( $30 < S < 31.2$ ) and (ii) smooth TS curves through  
the underlying water column ( $S > 31.2$ ) that appear to be unaffected by intrusive activity (Figures 4 and  
5a). For example, all stations from Region 3 exceeded the potential freezing temperature by  $\sim 0.1^\circ\text{C}$ ,  
205 while both stations from Region 2 show a similar regularity, but only exceed the potential freezing



temperature by  $\sim 0.03^{\circ}\text{C}$  (gray shaded area; Figure 5a). In contrast, all stations from Clusters II-V for the salinity/depth range of 30-31.2/20-65 m show temperatures that are relatively close to the potential temperature of freezing throughout the Halostad (gray shaded area; Figure 5b). We also note that the highest temperature offset from the potential freezing temperature is associated with CTD profiles from Region 3, which was ice-free during the preceding summer (Figure 2) and therefore warmed through solar heating. Region 2 was most recently ice-free during August 2013 (not shown), which likely led to the creation of a relatively warm subsurface layer. Thus, we subsequently refer to Cluster I as the “open water” cluster.

Cluster II (6 stations: SN15-8-11/66/68; Figure 7) is characterised by smooth *TS* curves slightly affected by intrusive activity (Figure 6), with water near the potential freezing temperature in the Halostad ( $S < 31.2$ ; gray shading in Figure 5). Within the Halocline, between salinities of 31.2 and 33.5 (Figure 6a, green shading) all profiles from this cluster are relatively warm, exceeding the mean curve by up to 1.5 standard deviations or  $0.07^{\circ}\text{C}$  (for  $\sigma_0 = 26 \text{ kg m}^{-3}$ ). In contrast, for  $S > 33.5$  this cluster is almost at the mean value (Figure 6a, pink shading). Stations from this cluster occupy the outer-shelf area (Region 1) near the middle of the glacial trough and were covered by multiyear landfast ice during our field program. In the following we assume that Cluster II represents the background oceanographic conditions over the Wandel Sea shelf, and subsequently refer to this group as the “basic” cluster.

Cluster III (6 stations: SN15-6/7/58/59/67/71; Figure 7) is characterized by temperatures that remain within 1 standard deviation through salinities between 31.2 and 33.5 (green shaded area, Figures 5 and 6a), except for two profiles that deviate from the mean by  $-0.1 \div -0.2^{\circ}\text{C}$  along the  $26.9 \pm 0.1 \text{ kg m}^{-3}$



isopycnal. In general, stations from Cluster III occupy almost the same area as Cluster II (Figure 7) and represent the transition from Cluster II, with smooth *TS* curves, to Cluster IV, strongly impacted by intrusive activity. Thus, we refer to this cluster as the “transit” cluster.

Cluster IV (6 stations: SN15-62-65/69/70; Figure 7) profiles display the most significant  
230 intrusive activity within the Halocline between salinities of 31.2 and 33.5 (Figures 5 and 6). Within this range all *TS* curves show negative temperature anomalies greater than one standard deviation for at least half of the  $0.1 \text{ kg m}^{-3}$  intervals (Figure 6a). In contrast, the profiles from this cluster have positive temperature anomalies of about one standard deviation throughout the underlying water where  $S > 33.5$ . Profiles from this cluster were taken over the compact area on the eastern flank of the glacial trough on  
235 the Wandel Sea outer shelf (Figure 7) and are the closest profiles to the continental slope. Hereafter we refer to these stations as the “intrusive” cluster.

Cluster V (4 stations: SN15-13/72/73/75; Figure 7) is characterized by profiles that (i) show exceptionally strong intrusive activity in the *TS* plot for  $33.5 < S < 33.85$  (90-100 m depth) and (ii) comprise a new mixing line for the underlying water layer ( $S > 33.85$ ,  $>100$  m depth) which is  
240 remarkably different from the ambient Clusters II-IV (Figure 6). For stations SN15-13/72/75, thermohaline intrusions show density-compensated negative salinity/temperature anomalies of up to  $-0.03/-0.32^\circ\text{C}$ , and exceed the mean by more than two standard deviations. Station SN15-73 shows smaller intrusions, but they still exceed the mean by about one standard deviation. For  $S > 33.9$ , profiles from this cluster align with a distinct mixing line that is shifted towards lower temperatures relative to  
245 the ambient profiles. Profiles from this cluster were collected near the front of the glacial tongue, thus we refer to this cluster as the “glacier” cluster.



## 4. Discussion

Below we discuss the potential origin and modifications of the water masses in each of the five  
250 clusters we have identified over the Wandel Sea shelf. We also use our findings to trace the Arctic  
Ocean outflow through western Fram Strait, putting our results into the context of upstream  
observations in the Canada Basin and downstream observations in the Northeast Water Polynya (NEW).

### 4.1. Interaction with tidewater glacier

We speculate that cluster V shows features that we attribute to the ocean-glacier interaction.  
These are (i) the abnormal intrusive activity at the base of the Halocline and (ii) the transition of profiles  
in the *TS* space towards a new mixing line for the underlying Atlantic modified PrW at the glacier front  
(Figure 6). The ambient water from Clusters II-IV exhibits a background mixing line between the  
Halocline and AW (Figure 5b) which seems to be unaffected by the ocean-glacier interaction. During  
260 summer, significant surface glacial runoff provides a new end-member to this mixture. However, during  
winter there is no surface glacial runoff, and subglacial runoff is negligible, as confirmed by our CTD  
profiles during April and May that show no surface salinity gradient around the termination of the  
glacier. Even though glacial melt water is negligible during winter, the glacier can still modify the  
ambient mixing line through ocean-glacier interactions as we will discuss below.

265 Water cools when it comes in contact with glacier ice that is colder than the *in situ* freezing  
point. For example, for the Ross Ice Shelf in Antarctica, *Wexler* [1960] reported the glacier ice  
temperature increased from  $-22^{\circ}\text{C}$  at the surface to  $-14^{\circ}\text{C}$  at 200 m depth and to  $-1.7^{\circ}\text{C}$  at the glacier-



ocean interface at ~260 m depth. For the Flade Isblink Ice Cap outlet, the cold glacier can significantly affect the water column below the floating glacier tongue, generating a new water mass that can be colder than the ambient PrW modified by interaction with the underlying warm AW. The sub-glacier freshwater discharge can also reduce the salinity of this water mass; however, the sub-glacier discharge is likely negligible during winter. For the floating glacier, a lateral interaction between the water below the glacier tongue and the Atlantic-modified PrW can (i) give rise to the intrusions we observed at the base of the Halocline layer and (ii) modify the background mixing line towards colder temperatures as also observed (Figures 5 and 6). Similar intrusive interleavings at the front of a tidewater glacier were reported by *Jacobs et al.* [1981], *Jenkins* [1998] and *Mayer et al.* [2000].

For station SN15-13, located ~200 m from the termination of the tidewater glacier (Figure 7), the CTD profile shows an intrusion of cool, turbid water between 88 and 97 m depths that caused a temperature inversion of  $-0.32^{\circ}\text{C}$  and a sharp increase in the water turbidity from 0.2 to 1.5 NTU (Figure 8). A similar rapid increase in turbidity with depth was also recorded at the Helheim Glacier in southeast Greenland [*Straneo et al.*, 2011]. We attribute this increase to the lower boundary of the glacier tongue at 88 m depth. In this case the turbid water can be attributed to subglacial discharge, or submarine melting of ice releasing sediments. The water dynamics (3-5 cm/s as a maximum) is too weak for resuspending the 20 m thick bottom layer. Assuming the ratio of glacier/water densities to be 0.917, we get a glacier elevation above the sea surface of ~7.5 m that corroborates with our visual estimates.

At the front of the glacier termination, the water below the depth of the glacier tongue is on average cooler by  $0.28^{\circ}\text{C}$  and less salty ( $\sim 0.2$ ) than the ambient water as measured at SN15-09 (Cluster



II; Figure 8), suggesting a lateral heat flux along with an insignificant sub-glacier fresh water discharge  
290 in winter and/or a remnant of the larger discharge during summer. We suggest that interaction between  
the ambient shelf water and water below the glacier tongue, modified in direct contact with glacier ice,  
deflects the mixing line between the Halocline and AW in the *TS* space towards a lower temperature  
and, to a lesser extent, to lower salinity values.

On the stations in cluster V, taken close to the tidewater glacier outlet, intrusions of colder, less  
295 saline water are observed around 90 m depth, which is the estimated lower boundary of the floating ice  
tongue. The water circulating below the glacier is initially warmer than the *in situ* freezing point of  
seawater and will be cooled as it gets in contact with the bottom of the glacier. The lost heat is partly  
used to melt ice and partly conducted into the glacier, increasing its temperature. Here we assume that  
the largest part of the heat goes to melting and we presently ignore the fraction of heat conducted into  
300 the glacier. We also ignore all other freshwater sources, e.g. runoff and seasonal ice melt, except that  
due to melting of the glacier by ocean heat from below. The density reduction of the ocean water due to  
added melt water is larger than the density increase due to cooling, and the less saline water will ascend  
along the lower boundary of the glacier, until it reaches the vertical terminus. At this point the water  
will penetrate into the ambient water column at its density level, forming colder, less saline isopycnal  
305 intrusions [e.g., *Magorrian and Wells, 2016*].

To describe the interactions occurring below the floating glacier to the first order we then  
assume that all heat lost by the water parcel is used to melt ice. The addition of meltwater leads to a  
salinity reduction  $\Delta S$  that can be estimated from:



$$\Delta S = \frac{S \frac{c_p \Delta T}{L}}{\left(1 - \frac{c_p \Delta T}{L}\right)}$$

310 Here  $c_p = 3980 \text{ J}^\circ\text{C}^{-1}\text{kg}^{-1}$  is the heat capacity of sea-water and  $L = 334500 \text{ Jkg}^{-1}$  is the latent heat of melting.  $\Delta T$  is the temperature reduction and  $S$  is the salinity of the water parcel re-emerging from underneath the glacier.

We do not have observations from below the floating glacier and we have to make assumptions both about the initial characteristics of the water entering below the glacier and the cooling and  
 315 reduction of the salinity that occur by interaction with the glacier. The salinity of the water re-entering the water column from below the glacier is  $S \sim 33.65$  and the observed temperature reduction, compared to the ambient profiles, is  $\Delta T \sim 0.3^\circ\text{C}$  (Figures 5b and 7). We know that the initial salinity then has to be higher than 33.65. Looking at the ambient profiles (Figure 4) we note that the mean temperature of the water that could possibly enter beneath the glacier is about  $-0.8^\circ\text{C}$ . Assuming it is cooled to freezing  
 320 temperature,  $\Delta T$  is  $1^\circ\text{C}$  and  $\Delta S$  becomes  $\sim 0.4$ . This gives an initial salinity of 34.05 to the water entering below the glacier.

However, the observed cold intrusions are not at the freezing point, instead they are warmer, around  $-1.4^\circ\text{C}$  (Figure 8). This could indicate that the water entering below the glacier is not cooled to the freezing point, but only by  $\sim 0.3^\circ\text{C}$ . The initial salinity would then be 33.8 rather than 34.05. Another  
 325 possibility is that the cold water penetrates isopycnally into the water column and becomes warmer and more saline by mixing with ambient water. Assuming that the intrusions are isopycnal, the changes in temperature and salinity due to mixing becomes:





$$\alpha\Delta T = \beta\Delta S$$

Here  $\alpha=0.4\times 10^{-4} \text{ }^{\circ}\text{K}^{-1}$  is the coefficient for the heat expansion around  $-1^{\circ}\text{C}$  and  $\beta=8\times 10^{-4} \text{ psu}^{-1}$  is the  
330 coefficient of salt contraction. A temperature change of  $0.5^{\circ}\text{C}$  then corresponds to a salinity change of  
0.025, making the salinity at the freezing point of 33.625, close to the observed 33.65 at the intrusion  
and giving the initial salinity as 34.025. This suggests that the intrusions observed on the stations close  
to the tidewater glacier outlet (Cluster V) might derive from the outflow of colder, less saline water  
335 masses.

#### 4.2. Interaction with ambient water from the continental slope

We use the occurrence of intrusive interleaving as a tracer for the shelf-slope interaction. The  
intrusive Halocline from Cluster IV was observed over the outer shelf (Figure 7) adjacent to the  
340 Greenland continental slope, where a water mass with different thermohaline properties is located  
(Figure 4). The intrusions are indications of isopycnal interaction between the Atlantic-modified  
Halocline occupied over the Wandel Sea shelf and a cooler PrW observed over the Wandel Sea  
continental slope (Figure 4). Within the depth range of the Halocline ( $\sim 65\text{-}100 \text{ m}$ ), the cooler PrW is  
likely maintained by a weakened upward heat flux from the deepened AW in the off-shelf area. Over  
345 the Wandel Sea shelf, the upper AW boundary was recorded at  $\sim 140 \text{ m}$ , while in June-July 2015 and  
August 2008 it was  $\sim 30 \text{ m}$  deeper over the adjacent continental slope (Figure 4). We note, however, that  
the water mass structure over the continental slope of Northeast Greenland shows significant



interannual variability [e.g., *Falck et al.*, 2005]. Overall, the distinct difference between the on-shelf and off-shelf water mass structure (Figure 4) suggests their different origins, which are further discussed in section 4.3.

In the following we speculate that the intrusive Halocline from Cluster IV is generated by interaction between the Atlantic-modified shelf Halocline (Cluster II) and the PrW from the continental slope as shown in Figure 9a. We suggest that this interaction is isopycnal because all intrusions are density compensated. For the Halocline layer over the southern Wandel Sea continental slope, *Rudels et al.* [2005] reported an intrusive interleaving conditioned by isopycnal interaction between relatively warm Halocline water from the upper continental slope, and cold PrW from the lower continental slope.

For further interpretation of our results on the shelf-slope interaction we include 184 CTD profiles taken between 1992 and 1993 in the NEW area [*Bignami and Hopkins*, 1997; *Budéus et al.*, 1997; *Falck*, 2001], which is downstream from the Wandel Sea shelf (Figures 1 and 2b). The *TS* curves from the NEW area show two distinct modes: (i) the polynya (shelf) mode, which is similar to the “basic” Cluster II derived for the Wandel Sea shelf (Figure 5b, 6 and dark blue lines in Figure 9a) except for a slightly colder ( $\sim 0.05^{\circ}\text{C}$ ) and saltier ( $\sim 1$ ) low Halostad, and (ii) the continental slope mode, which within the salinity range of the Wandel Sea shelf Halocline (31.2-34) shows a completely different shape of the *TS* curve (red lines in Figure 9a). Specifically the *TS* line of the continental slope mode extends linearly through the Halostad to salinity of  $\sim 34$  (red dashed line in Figure 9a; red rectangles in Figure 9b), maintaining temperatures relatively close to the surface freezing temperature (blue dashed line Figure 9b).



For the NEW area, the remarkable difference between the polynya (shelf mode) and the continental slope mode was also reported by *Straneo et al.* [2012] and *Wilson and Straneo* [2015], with a *TS* structure similar to the one presented in Figure 9 (Figure 3 from *Wilson and Straneo*, 2015). Moreover, for the 79N glacier outlet (Figure 2b), *Straneo et al.* [2012] used the upper continental slope CTDs as ambient stations and compared them to CTD profiles taken through a rift in the floating glacier tongue (see Figure 2b for the glacier station position). For the water layer at ~40-90 m depth, they reported ambient water that was saltier than water below the glacier tongue by ~1-2, attributing this difference to the sub-glacier water discharge. We note, however, that this freshening is of the same magnitude as the salinity difference between the shelf Halostad/Halocline and the continental slope PrW (Figure 9). Thus, freshening reported by *Straneo et al.* [2012] could be alternatively explained by the occurrence of the Halostad-like freshened water layer below the glacier tongue.

In the following sections 4.3 and 4.4, we use the differences between the on-shelf and off-shelf water mass structures and the similarities between the Wandel Sea and NEW areas to trace the origin of the Halostad, Halocline and AW in the Wandel Sea and their modification along the northeast Greenland coast.

#### 4.3. Tracing the origin of the Wandel Sea Halostad, Halocline and AW: Local source

The distinct difference between the on-shelf and off-shelf water mass structure and disposition suggests they have different origins and/or pathways to the Wandel Sea shelf and continental slope. The occurrence of the shelf Halostad can be explained by local freshening by summer snow/sea-ice melt water and freshwater from the glacier runoff. In turn, the uplifted on-shelf Atlantic-modified PrW and



AW can originate from local modifications due to upwelling of AW over the Wandel Sea continental  
390 slope.

The under-ice surface layer over the Wandel Sea shelf is significantly freshened, potentially  
providing a source of freshwater for the freshened Halostad over the shelf if vertical mixing overcomes  
the salinity (density) stratified sub-surface halocline as was suggested for NEW by *Bignami and  
Hopkins* [1997]. Among the Arctic shelves, the Wandel Sea sub-surface halocline shows exceptionally  
395 strong vertical stratification with salinity increasing from 18 to 30 across a ~10 m thick sub-surface  
halocline layer during winter (Figure 4). This is comparable to the Laptev Sea shelf where strong  
salinity stratification is maintained by the river runoff from the Lena River, the second largest river  
flowing into the Arctic Ocean [e.g., *Dmitrenko et al.*, 2010]. *Dmitrenko et al.* [2012] showed that  
significant velocity shear over the Laptev Sea shelf, attributed to the lunar semidiurnal baroclinic  
400 internal tide M2 with velocity ~15 cm/s at 11 m and ~7 cm/s at 19 m depth is required to transform the  
vertically stratified water into a locally mixed layer. In contrast, over the Wandel Sea shelf velocities  
hardly exceed 3-5 cm s<sup>-1</sup>. The Acoustic Doppler current profiler data from the mooring temporarily  
deployed at SN15-13 revealed that the most energetic M2 tidal currents are weak, decreasing from ~2  
cm/s beneath the ice to ~1 cm/s below 60 m depth [*Sergei Kirillov, pers. comm.*, 2016]. Moreover, the  
405 multiyear landfast ice cover over the Wandel Sea shelf precludes the wind stress from vertically mixing  
the stratified water column.

Hypothetically, the wind-driven upwelling of the Atlantic-modified PrW and AW over the  
continental slope can result in uplift of the water masses over the outer shelf. In this case, however, the  
shallowing of the Atlantic-modified PrW and the upper boundary of AW is accompanied by on-shelf



410 inflow of the deeper and saltier water from the continental slope. In contrast, the Atlantic-modified Halocline on the shelf is less salty compared to ambient water from the continental slope by  $\sim 1-2$ .

In the following we discuss our results in the context of upstream observations in the Canada Basin (e.g., Figure 10) and downstream observations in the NEW region.

#### 415 **4.4. Tracing the origin of the Wandel Sea Halostad, Halocline and AW: Far field advection**

We suggest that the on-shelf Halostad and the associated Halocline can be advected from the remote upstream areas where sources of fresh water exist. Similarly, as with the shelf Halostad, the shallower AW layer recorded over the Wandel Sea shelf and the deeper AW layer found over the continental slope should be attributed to the different branches of the AW outflow from the Arctic  
420 Ocean through western Fram Strait.

The East Greenland Current carries the Arctic Ocean outflow through western Fram Strait southward along the Greenland shelf and continental slope – Figure 1 [e.g., *Rudels et al.*, 2002; *Jeansson et al.*, 2008]. It transports cold, low salinity Polar surface waters with  $\sigma_0 \leq 27.7 \text{ kg m}^{-3}$  [*Rudels et al.*, 2002] that are comprised of the river runoff and net precipitation water, but also of the  
425 less saline PcW that enters the Arctic Ocean through Bering Strait [*Jones et al.*, 1998, 2003, 2008; *Rudels et al.*, 2002; *Falck et al.*, 2005; *de Steur et al.*, 2009; *Sutherland et al.*, 2009] – Figure 1. PcW within the Arctic Ocean is generally assigned to water with  $S \leq 33$  [*von Appen and Pickart*, 2012] and has both a summer and winter signature based on its formation. The summer PcW with temperatures above  $-1.2^\circ\text{C}$  and salinities between 31 and 32 [*Steele et al.*, 2004] is usually comprised of the Chukchi  
430 Summer Water [*Woodgate et al.*, 2005] and the Alaskan Coastal Water [*Pickart et al.*, 2005]. Below the



summer PcW is a layer of winter PcW that can be as cold as  $-1.45^{\circ}\text{C}$  and forms during sea ice formation within the Bering and Chukchi Seas [Jones and Anderson, 1986; Weingartner et al., 1998; Pickart et al., 2005].

It has been shown that the subsurface layer over the eastern Greenland coast is comprised of the  
435 PcW outflow from the Arctic Ocean [Jones et al., 1998, 2003, 2008; Falck, 2001; Falck et al., 2005; Jeansson et al., 2008; Sutherland et al., 2009]. For the 1993 observations over the NEW shelf area, in the subsurface Halostad layer down to  $\sim 80$  m depth, an average of about 90% is found to have Pacific origin [Falck, 2001]. This result by Falck [2001] brought a different mechanism of the Halostad formation to light. In contrast to Bignami and Hopkins [1997], Falck [2001] insists on an upstream  
440 Pacific source for the Halostad water and underlying Halocline, rather than a local origin.

Upstream over the Canada Basin, PcW impacts the halocline structure, producing a double halocline with a “cold Halostad” formed by the volumetric injection of the winter PcW that overlies Low Halocline Water of the Eurasian Basin origin [McLaughlin et al., 2004; Shimada et al., 2005]. The salinity range of the cold Halostad in the Canada Basin occupies  $31.5 < S < 33.5$  with the lowest  
445 temperature of  $\sim -1.7^{\circ}\text{C}$  at the base of the Halostad indicating the winter PcW [McLaughlin et al., 2004; Shimada et al., 2005]. This water mass structure resembles that for the eastern Beaufort Sea continental slope (Figure 10).

In general, the Halostad structure over the Canada Basin and adjoining continental margin is similar to that recorded over the Wandel Sea shelf (Figure 4). However, over the Wandel Sea shelf the  
450 Halostad is cooler and fresher (Figure 10c) occupying a salinity range of  $30.0 < S < 31.5$ . The Wandel Sea Halostad is also shallower (15-65 m depth versus  $\sim 50$ -200 for the Canada Basin). The different



salinity range of the Halostad in the Wandel Sea and Canada Basin suggests that significant modifications occurred during transit of the winter PcW from the Bering and Chukchi Seas to the Wandel Sea. It seems that the winter PcW is modified by vertical mixing with overlaying summer PcW and/or river runoff accumulated in the Canada Basin. For example, *Jones et al.* [2008] revealed that over the northeast Greenland coast at  $\sim 81^\circ\text{N}$ , the PcW fraction is comparable with the river water fraction. Moreover, water from the Siberian shelves, especially the Laptev Sea shelf also has the same salinity and temperature range and can mix into and cool the summer PcW [e.g., *Dmitrenko et al.*, 2011]. This assumes that the river water impacts a Wandel Sea Halostad initially comprised of the winter PcW.

The remote origin of the Halostad is also confirmed by the elevated values of the CDOM fluorescence through the Halostad layer at station SN15-13 (Figure 8). The CDOM fluorescence is a good tracer of the Arctic Ocean terrigenous organic matter primarily attributed to the Eurasian and American continental runoff water [e.g., *Granskog et al.*, 2012] as well as to interactions with sediments on the Arctic shelves [e.g., *Guéguen et al.*, 2007]. The CDOM fluorescence maxima in the Halostad at station SN15-13 is consistent with results from the Canada Basin where this maxima is attributed to the winter PcW [e.g., *Guéguen et al.*, 2007] and the continental river runoff water [e.g., *Granskog et al.*, 2012]. For the downstream NEW area, *Amon et al.* [2003] also reported the intermediate maxima of the CDOM fluorescence through the shelf Halostad layer (Figure 9a from *Amon et al.*, 2003). The glacier melt water provides the low CDOM contribution, which is comparable to background low levels in AW [Stedmon et al., 2015]. Overall, this confirms the remote origin of the Halostad layer over the Wandel



Sea shelf and strengthens our discussion on the modification of the Pacific-derived Halostad by river runoff while en route from the Canada Basin to Fram Strait.

As the Halocline and AW move along the Canada Basin margins toward northern Greenland,  
475 they ascend in the water column from 100-200 m and 220-320 m in the Canada Basin [*McLaughlin et al.*, 2004; *Shimada et al.*, 2005] to 85 m and 140 m on the Wandel Sea shelf, respectively (Figure 4). Following *Rudels et al.* [2004], we speculate that this rise is due to the gradual thinning of the low salinity layer above. The thinning could be caused by the upper layer either being confined to the Beaufort Gyre or draining through the Canadian Arctic Archipelago and ultimately into Baffin Bay  
480 [*Rudels et al.*, 2004]. This is consistent with a gradual shallowing of the upper boundary of AW traced by isopycnal  $\sigma_0 = 27.4 \text{ kg m}^{-3}$  from  $\sim 230$  m in the Canada Basin to  $\sim 140$  m in the Wandel Sea [*Polyakov et al.*, 2010].

The occurrence of the Pacific origin Halostad along the northeast Greenland coast suggests that PcW is transported southward by a narrow coastal branch of the East Greenland Current. This current  
485 also advects a shallowed AW, which likely originated from the Canada Basin branch (Figure 1). The cross-slope interaction between the coastal and off-shelf branches of the East Greenland Current gives rise to the intrusive interleaving observed over the Wandel Sea outer shelf (Figure 6a).

## 5. Summary and conclusions

490 The first-ever CTD observations over the Wandel Sea shelf and continental slope were collected in April-May and June-July 2015, respectively. We use CTD profiles deeper than 100 m to focus on the origin of water masses, and to identify interactions between the shelf and slope, and between the ocean





and outlet glaciers entering the Wandel Sea. The stations taken on the Wandel Sea shelf and farther to the east on the Greenland slope reveal two pathways for the advected water masses, one over the shelf  
495 and one along the continental slope. The one over the slope has warm, saline AW lying below a deep, cold, less saline and fairly homogenous upper layer that is capped by low salinity surface water created by seasonal ice melt and heated by solar radiation. This suggests that AW recirculating within the Eurasian Basin (Figure 1) with the less dense upper layer initially formed by sea ice melt water are mixed into the upper part of the entering AW. In the Nansen Basin this layer is homogenized by haline  
500 convection each winter [Rudels *et al.*, 1996].

The water column found on the shelf has much colder and less saline AW located closer to the surface than the AW over the slope. The AW characteristics here are similar to those observed at much greater depth in the Canada Basin, indicating that this AW has circulated around the entire deep Arctic basins and now is returning towards Fram Strait. In the Canada Basin, the AW is covered by the  
505 halocline layer and it is comprised of both Atlantic ( $S \sim 34$ ) and Pacific derived water, especially the Pacific Winter Water, with  $S \sim 33.1$  [e.g., Jones and Anderson, 1986], as well as other low salinity waters. These low salinity waters lie shallower than the sill depth of the Canadian Arctic Archipelago and can pass through the straits into Baffin Bay. This would cause the AW to rise in the water column as it moves along the northern Canadian coast, until it is shallow enough to flow over deeper shelves  
510 like that of the Wandel Sea.

Over the Wandel Sea shelf, the Pacific Winter Water, that was so distinct in the Canada Basin, seems to be either missing or only occupying a narrow depth range. Instead the coldest water is found in the Halostad with salinity around 31 instead of 33. The low salinity upper layer and the thick ice cover



in winter preclude the local homogenization of the water column down to the Halostad. Thus, the  
515 Halostad must be advected from elsewhere. A conceivable scenario could be that most of the PcW  
drains out of the Arctic Ocean through the Canadian Arctic Archipelago. This likely makes the AW  
ascend and it would allow water from the Polar Mixed Layer, of Atlantic or Pacific origin, circulating in  
the Beaufort Gyre and in the Arctic basins to replace the water leaving through the straits in the  
archipelago and penetrate onto the shelf, creating a different upper layer above the AW.

520 Our findings are summarised as follows:

(i) The sub-surface (15-70 m depth) “cold Halostad” layer with salinities of 30-31.5 and  
associated underlying Halocline layer is a distinct feature of the Wandel Sea shelf hydrography. It does  
not persist over the Wandel Sea continental slope, indicating the water masses over the shelf and slope  
have different origins. A similar water mass structure was observed downstream in the Northeast Water  
525 Polynya area. This structure is likely maintained by the coastal branch of the Pacific Water outflow  
from the Arctic Ocean, modified by interaction with river runoff over the upstream Canada Basin.

(ii) The Halocline layer centered at ~80 m (salinity of ~33) separates the Pacific-origin cold  
Halostad from the Polar Water, modified by interaction with warm Atlantic water outflow from the  
Arctic Ocean through western Fram Strait. The upper boundary of the Atlantic Water ( $T \sim 0^{\circ}\text{C}$ ) is  
530 recorded at ~170 m depth on the continental slope and ~30 m shallower over the adjoining shelf. This  
difference suggests that, as with the subsurface layer, the intermediate water over the shelf and  
continental slope is conditioned by different branches of the Atlantic water outflow from the Arctic  
Ocean.



(iii) The lateral shelf-slope interaction between on-shelf relatively warm Atlantic-modified  
535 Halocline water and off-shelf cold Polar Water gives rise to the intrusive interleaving observed over the  
Wandel Sea outer shelf.

(iv) At the base of the Halocline layer, cold and turbid water intrusions were recorded at the  
front of the tidewater glacier outlet. The temperature-salinity plots of the CTD profiles from this region  
show a mixing line that is deflected relative to the ambient water. Both features are likely conditioned  
540 by the ocean-glacier interaction.

In summary, our analysis suggests the existence of a coastal branch of the East Greenland  
Current advecting Pacific Water of Arctic origin southward along the northeast Greenland coast. This is  
consistent with an earlier proposition by *Rudels et al.* [2004], downstream observations along the  
southeast coast of Greenland [e.g., *Bacon et al.*, 2002; *Sutherland and Pickart*, 2008; *Sutherland et al.*  
545 2009] and numerical simulations [*Hu and Myers*, 2013; *Aksenov et al.*, 2016]. Finally, we note that our  
observations were not accompanied by water sampling for determining the nitrate/phosphate  
relationship commonly used to trace the Pacific Water in the Arctic Ocean and Greenland Sea. This  
deficiency in the observational program conducted clearly shows the necessity for further research in  
this area using advanced methods of tracer analysis.

550  
**Acknowledgments:** This study was funded by the Canada Excellence Research Chair program (SR),  
the Canada Research Chair program (DB), the Canada Foundation of Innovation, the National Sciences  
and Engineering Research Council of Canada (grant RGPIN-2014-03606, ID), the Manitoba Research  
and Innovation Fund, the University of Manitoba, Aarhus University, the Greenland Institute of



555 Natural Resources, and the EU project NACLIM (grant agreement 308299, BR). We thank Ivali  
Lennert, Kunuk Lennert and Egon Frandsen for technical assistance in the field. We also appreciate  
outstanding logistical support from the Station Nord Danish military personnel. John Mortensen  
(Greenland Climate Research Centre) provided valuable comments on the ocean-glacier interaction.  
Comments and editing by Dr. John K. Hall, the owner of the research hovercraft SABVABAA, are  
560 highly appreciated. Dr. Nils Nørgaard-Pedersen kindly provided bathymetric data used in Figure 3. This  
work is a contribution to the Arctic Science Partnership (ASP) and the ArcticNet Networks of Centres  
of Excellence programs. For the Wandel Sea CTD data contact ID at igor.dmitrenko@umanitoba.ca

## Reference

- 565 Aksenov, Y., et al. (2016), Arctic pathways of Pacific Water: Arctic Ocean Model Intercomparison  
experiments, *J. Geophys. Res. Oceans*, 121, 27–59, doi:10.1002/2015JC011299.
- Amon, R. M. W., G. Bude'us, and B. Meon (2003), Dissolved organic carbon distribution and origin in  
the Nordic Seas: Exchanges with the Arctic Ocean and the North Atlantic, *J. Geophys. Res.*, 108(C7),  
3221, doi:10.1029/2002JC001594.
- 570 Bacon, S., G. Reverdin, I. G. Rigor, and H. M. Smith (2002), A freshwater jet on the east Greenland  
shelf, *J. Geophys. Res.*, 107(C7), 3068, doi:10.1029/2001JC000935.
- Bignami, F. and T. S. Hopkins (1997), The water mass characteristics of the Northeast Water Polynya:  
Polar Sea data 1992–1993, *J. Marine Sys.*, 10, 139-156.
- 575 Budéus, G., W. Schneider and G. Kattner (1997), Distribution and exchange of water masses in the  
Northeast Water polynya (Greenland Sea), *J. Marine Sys.*, 10, 139-156.
- de Steur, L., E. Hansen, R. Gerdes, M. Karcher, E. Fahrbach, and J. Holfort (2009), Freshwater fluxes  
in the East Greenland Current: A decade of observations, *Geophys. Res. Lett.*, 36, L23611,  
doi:10.1029/2009GL041278.
- 580 Dmitrenko, I. A., S. A. Kirillov, T. Krumpfen, M. Makhotin, E. P. Abrahamsen, S. Willmes, E.  
Bloskinab, J. A. Hölemann, H. Kassens and C. Wegner (2010), Wind-driven diversion of summer river



- runoff preconditions the Laptev Sea coastal polynya hydrography: Evidence from summer-to-winter hydrographic records of 2007–2009, *Continental Shelf Research*, 30(15), 1656–1664, doi:10.1016/j.csr.2010.06.012.
- 585 Dmitrenko, I. A., V. V. Ivanov, S. A. Kirillov, E. L. Vinogradova, S. Torres-Valdes, and D. Bauch (2011), Properties of the Atlantic derived halocline waters over the Laptev Sea continental margin: Evidence from 2002 to 2009, *J. Geophys. Res.*, 116, C10024, doi:10.1029/2011JC007269.
- Dmitrenko, I. A., S. A. Kirillov, E. Bloshkina, and Y.-D. Lenn (2012), Tide-induced vertical mixing in the Laptev Sea coastal polynya, *J. Geophys. Res.*, 117, C00G14, doi:10.1029/2011JC006966.
- 590 Dmitrenko, I. A., S. A. Kirillov, A. Forest, Y. Gratton, D. L. Volkov, W. J. Williams, J. V. Lukovich, C. Belanger, and D. G. Barber (2016), Shelfbreak current over the Canadian Beaufort Sea continental slope: Wind-driven events in January 2005, *J. Geophys. Res. Oceans*, 121, 2447–2468, doi:10.1002/2015JC011514.
- Eicken, H. (1994), Structure of under-ice melt ponds in the central Arctic and their effect on the sea-ice cover, *Limnol. Oceanogr.*, 39(3), 682–694.
- 595 Falck, E. (2001), Contribution of waters of Atlantic and Pacific origin in the Northeast Water Polynya, *Polar Res.*, 20(2), 193–200.
- Falck, E., G. Kattner, and G. Bude'us (2005), Disappearance of Pacific Water in the northwestern Fram Strait, *Geophys. Res. Lett.*, 32, L14619, doi:10.1029/2005GL023400.
- 600 Flocco, D., D. L. Feltham, E. Bailey, and D. Schroeder (2015), The refreezing of melt ponds on Arctic sea ice, *J. Geophys. Res.*, 120, 647–659, doi:10.1002/2014JC010140.
- Granskog, M. A., C. A. Stedmon, P. A. Dodd, R. M. W. Amon, A. K. Pavlov, L. de Steur, and E. Hansen (2012), Characteristics of colored dissolved organic matter (CDOM) in the Arctic outflow in the Fram Strait: Assessing the changes and fate of terrigenous CDOM in the Arctic Ocean, *J. Geophys. Res.*, 117, C12021, doi:10.1029/2012JC008075.
- 605 Gade, H. G. (1979), Melting of ice in sea water: A primitive model with application to the Antarctic Ice Shelf and iceberg, *J. Phys. Oceanogr.*, 9, 189–98.
- Guéguen, C., L. Guo, M. Yamamoto-Kawai, and N. Tanaka (2007), Colored dissolved organic matter dynamics across the shelf-basin interface in the western Arctic Ocean, *J. Geophys. Res.*, 112, C05038, doi:10.1029/2006JC003584.
- 610 Hu, X. and P. G. Myers (2013), A Lagrangian view of Pacific water inflow pathways in the Arctic Ocean during model spin-up, *Ocean Modelling*, 71, 66–80, doi:10.1016/j.ocemod.2013.06.007.



- Jeansson, E., S. Jutterström, B. Rudels, L. G. Anderson, K. A. Olsson, E. P. Jones, W. M. Smethie Jr. and J. H. Swift (2008), Sources to the East Greenland Current and its contribution to the Denmark Strait Overflow, *Progress in Oceanography*, 78, 12-28, doi: 10.1016/j.pocean.2007.08.031
- 615 Jenkins, A. (1999), The impact of melting ice on ocean waters, *J. Phys. Oceanogr.*, 29(9), 2370-2381.
- Jones, E. P. and L. G. Anderson (1986), On the origin of the chemical properties of the Arctic Ocean halocline, *J. Geophys. Res.*, 91, C9, 10,759-10,767, doi: 10.1029/JC091iC09p10759.
- Jones, E. P., L. G. Anderson, and J. H. Swift (1998), Distribution of Atlantic and Pacific waters in the upper Arctic Ocean: Implications for circulation, *Geophys. Res. Lett.*, 25, 765-768.
- 620 Jones, E. P., J. H. Swift, L. G. Anderson, M. Lipizer, G. Civitarese, K. K. Falkner, G. Kattner and F. A. McLaughlin (2003), Tracing Pacific water in the North Atlantic Ocean, *J. Geophys. Res.* 108(C4), 3116, doi: 10.1029/2001JC001141.
- Jones, E. P., L. G. Anderson, S. Jutterström and J. H. Swift (2008), Sources and distribution of fresh water in the East Greenland Current, *Progress in Oceanography*, 78, 37-44, doi:10.1016/j.pocean.2007.06.003.
- 625 Kattner, G. (2009), The Expedition of the Research Vessel "Polarstern" to the Arctic in 2008 (ARK-XXIII/2), *Berichte zur Polarforschung*, 590, 88 p.
- Magorrian, S. J., and A. J. Wells (2016), Turbulent plumes from a glacier terminus melting in a stratified ocean, *J. Geophys. Res. Oceans*, 121, 4670-4696, doi:10.1002/2015JC011160.
- 630 McLaughlin, F. A., E. C. Carmack, R. W. MacDonald, H. Melling, J. H. Swift, P. A. Wheeler, B. F. Sherr and E. B. Sherr (2004), The joint roles of Pacific and Atlantic-origin waters in the Canada Basin, 1997-1998, *Deep Sea Res. Part I*, 51, 107-128.
- Mayer, C., N. Reeh, F. Jung-Rothenhausler, P. Huybrechts, and H. Oerter (2000), The subglacial cavity and implied dynamics under Nioghalvfjærdsfjorden Glacier, NE-Greenland, *Geophys. Res. Lett.*, 27(15), 2289-2292.
- 635 Nørgaard-Pedersen, N., N. Mikkelsen and Y. Kristoffersen (2008), Late glacial and Holocene marine records from the Independence Fjord and Wandel Sea regions, North Greenland, *Polar Res.*, 27, 209-221, doi:10.1111/j.1751-8369.2008.00065.x.
- Palmer, S. J., A. Shepherd, A. Sundal, E. Rinne, and P. Nienow (2010), InSAR observations of ice elevation and velocity fluctuations at the Flade Isblink ice cap, eastern North Greenland, *J. Geophys. Res.*, 115, F04037, doi:10.1029/2010JF001686.
- 640



- Pickart, R.S., T. J. Weingartner, L. J. Pratt, S. Zimmermann and D. J. Torres (2005), Flow of winter-transformed Pacific water into the western Arctic, *Deep-Sea Res. II*, 52, 3175–3198.
- 645 Polyakov, I. V., L. A. Timokhov, V. A. Alexeev, S. Bacon, I. A. Dmitrenko, L. Fortier, I. E. Frolov, J.-C. Gascard, E. Hansen, V. V. Ivanov, S. Laxon, C. Mauritzen, D. Perovich, K. Shimada, H. L. Simmons, V. T. Sokolov, M. Steele and J. Toole (2010), Arctic Ocean warming contributes to reduced polar ice cap, *J. Physical Oceanography*, 40(12), 2743-2756, doi: 10.1175/2010JPO4339.1.
- 650 Rudels, B., E. P. Jones, L. G. Anderson, and G. Kattner (1994), On the intermediate depth waters of the Arctic Ocean, In: *The Polar Oceans and Their Role in Shaping the Global Environment: The Nansen Centennial Volume, Geophys. Monogr. Ser.*, vol. 849 85, Johannessen, O. M., R. D. Muench, and J. E. Overland (Eds.), pp. 33-46, AGU, Washington, D. C.
- Rudels, B., E. Fahrbach, J. Meincke, G. Budéus and P. Eriksson (2002), The East Greenland Current and its contribution to the Denmark Strait overflow, *ICES Journal of Marine Science*, 59, 1133–1154, doi:10.1006/jmsc.2002.128.
- 655 Rudels, B., E. P. Jones, U. Schauer and P. Eriksson (2004), Atlantic sources of the Arctic Ocean surface and halocline waters, *Polar Res.*, 23(2), 181–208.
- Rudels, B., G. Björk, J. Nilsson, P. Winsor, I. Lake and C. Nohr (2005), The interaction between waters from the Arctic Ocean and the Nordic Seas north of Fram Strait and along the East Greenland Current: results from the Arctic Ocean-02 Oden expedition, *Journal of Marine Systems*, 55, 1–30, doi:10.1016/j.jmarsys.2004.06.008.
- 660 Rudels, B. (2012), Arctic Ocean circulation and variability – advection and external forcing encounter constraints and local processes, *Ocean Sci.*, 8, 261–286, doi:10.5194/os-8-261-2012.
- Rinne, E. J., A. Shepherd, S. Palmer, M. R. van den Broeke, A. Muir, J. Ettema, and D. Wingham (2011), On the recent elevation changes at the Flade Isblink Ice Cap, northern Greenland, *J. Geophys. Res.*, 116, F03024, doi:10.1029/2011JF001972.
- 665 Shimada, K., M. Itoh, S. Nishino, F. McLaughlin, E. Carmack, and A. Proshutinsky (2005), Halocline structure in the Canada Basin of the Arctic Ocean, *Geophys. Res. Lett.*, 32, L03605, doi:10.1029/2004GL021358.
- 670 Straneo, F., R. G. Curry, D. A. Sutherland, G. S. Hamilton, C. Cenedese, K. Våge and L. A. Stearns (2011), Impact of fjord dynamics and glacial runoff on the circulation near Helheim Glacier, *Nature Geoscience*, 4, 322–327, doi:10.1038/ngeo1109.





- Straneo, F., D. Sutherland, D. Holland, C. Gladish, G. S. Hamilton, H. L. Johnson, E. R. Ringot, Y. Xu and M. Koppes (2012), Characteristics of ocean waters reaching Greenland's glaciers, *Annals of Glaciology*, 53(60), 202-210, doi:10.3189/2012AoG60A059.
- 675 Stedmon, C. A., M. A. Granskog, and P. A. Dodd (2015), An approach to estimate the freshwater contribution from glacial melt and precipitation in East Greenland shelf waters using colored dissolved organic matter (CDOM), *J. Geophys. Res. Oceans*, 120, 1107–1117, doi:10.1002/2014JC010501.
- Sutherland, D. A., and R. S. Pickart (2008), The East Greenland Coastal Current: Structure, variability, and forcing, *Prog. Oceanogr.*, 78(1), 58-77, doi:10.1016/j.pocean.2007.09.006.
- 680 Sutherland, D. A., R. S. Pickart, E. Peter Jones, K. Azetsu-Scott, A. Jane Eert, and J. Ólafsson (2009), Freshwater composition of the waters off southeast Greenland and their link to the Arctic Ocean, *J. Geophys. Res.*, 114, C05020, doi:10.1029/2008JC004808.
- von Appen, W.-J. and R. S. Pickart (2012), Two Configurations of the Western Arctic Shelfbreak Current in Summer, *J. Phys. Oceanogr.* 42, 329-351, doi: 10.1175/JPO-D-11-026.1.
- 685 Walsh, D. and E. Carmack (2003), The nested structure of Arctic thermohaline intrusions, *Ocean Modelling*, 5(3), 267–289, doi:10.1016/S1463-5003(02)00056-2.
- Weingartner, T., D. Cavalieri, K. Aagaard, and Y. Sasaki (1998), Circulation, dense water formation, and outflow on the northeast Chukchi shelf, *J. Geophys. Res.*, 103 (C4), 7647-7661.
- Wilson, N. J., and F. Straneo (2015), Water exchange between the continental shelf and the cavity beneath Nioghalvfjærdsbræ (79 North Glacier), *Geophys. Res. Lett.*, 42, 7648–7654, doi:10.1002/2015GL064944.
- 690 Woodgate, R. A., K. Aagaard, J. H. Swift, W. M. Smethie Jr., and K. K. Falkner (2007), Atlantic water circulation over the Mendeleev Ridge and Chukchi Borderland from thermohaline intrusions and water mass properties, *J. Geophys. Res.*, 112, C02005, doi:10.1029/2005JC003416.
- 695 Woodgate, R. (2013), Arctic Ocean Circulation: Going Around At the Top Of the World, *Nature Education Knowledge*, 4(8), 8.
- Wexler, H. (1960), Heating and melting of floating ice shelves, *J. Glaciology*, 3, 626-645.





## Tables

**Table 1:** The Wandel Sea water mass structure below 15 m depth

Water layer	Acronym	Property range (from/to)			
		Depth, m	Temperature, °C	Salinity	$\sigma_0$ , kg m <sup>-3</sup>
Halostad (of Pacific origin)	-	~ 15 / 65	~ -1.5 / -1.75	30/31.2	24.1/25.1
Pacific Water	PcW	PcW comprises the Halostad			
Halocline	-	~ 65 / 100	~ -1.75 / -0.65	31.2/34	25.1/27.3
Atlantic-modified Polar Water	PrW	~100 / 140	-1.15 / 0	34/34.5	27.3/27.7
Atlantic Water	AW	>140	>0 (up to 0.3)	>34.5	>27.7

700

**Table 2:** Description of the Wandel Sea CTD clusters

Cluster #	Cluster name	Station #	Main features	Property range (from/to)			
				Depth m	Temp. °C	Salinity	$\sigma_0$ kg m <sup>-3</sup>
I	Open water	31, 35, 53, 54, 79-83	“Warm” Halostad	15 / 65	~ -1.6	30.0 / 31.2	24.2 / 25
			Smooth TS curves	> 65	-1.7 / -0.8	> 31.2	> 25
II	Basic	8-11, 66, 68	“Cold” Halostad	15 / 65	-1.6 / -1.72	30.0 / 31.2	24.2 / 25
			Smooth TS curves	> 65	-1.7 / -0.8	> 31.2	> 25
III	Transit	6, 7, 58, 59, 67, 71	Moderate intrusions with temperature anomalies < 1 standard deviation	65 / 90	-1.25 / -1.6	31.2 / 33.5	25.6 / 26.7
IV	Intrusive	62-65, 69, 70	Significant intrusions with negative temperature anomalies > 1 standard deviation	65 / 90	-1.25 / -1.7	31.2 / 33.5	25.3 / 26.7



V	Glacier	13, 73, 73, 75	Significant intrusions	90 / 100	-1.2 / -1.4	33.5 / 33.85	>27.1
			Deflected mixing line	> 100	> -1.2	> 33.85	> 27.2

### Figure captions

**Figure 1:** Schematic circulation of the Atlantic Water (AW, red arrows) and Pacific Water (PcW, white arrows) in the Arctic Ocean and adjoining Greenland Sea following *Rudels et al.* [1994], *Jones* [2001], *Rudels* [2012], and *Woodgate* [2013]. The dashed and dotted red arrows correspond to the Fram Strait and Barents Sea branches of the AW inflow, respectively. The pink arrow indicates the East Greenland Current. The red dot depicts the position of Station Nord in Northeast Greenland.

**Figure 2:** (a) Station Nord (SN) on the Greenland map. The pink shading highlights the Wandel Sea region with adjoining fjord system, Flade Isblink Ice Cap (FIIC), the Northeast Water Polynya (NEW) area and the 79 North Glacier outlet enlarged in panel (b). (b) The MODIS/TERRA satellite image from 22 August 2014 taken over the SN/FIIC/NEW area. Red and black circled crosses indicate the CTD stations occupied over the Wandel Sea outer-shelf during the ARKXXIII/2 expedition in August 2008 and in a rift in the 79 North Glacier in August 2009. Red crosses depict the CTD stations occupied in June-July 2015 over the Wandel Sea continental slope (> 1000 m depth) during the Norwegian FRAM 2014-15 sea ice drift. The dashed black rectangle indicates the 2014 study area shown in Figure 3. Red/yellow/blue dashed rectangles depict regions 1/2/3, respectively, with depth exceeding 100 m.

**Figure 3:** The Sentinel-1 C-SAR image from 2 February 2015 with the CTD stations overlaid. The dark areas along the coast are associated with first year landfast ice (< 1.8 m thick). The lighter areas indicate



720 the multi-year landfast ice (~2 m to > 4 m thick). White and black circles identify stations with CTD  
 (April-May 2015) and depth (May 2006, adopted from *Nørgaard-Pedersen et al.* [2008] and April  
 2015) measurements, respectively, with depths shown by color. CTD stations > 100 m deep are  
 identified by their station numbers. Blue arrows indicate the northern outlet glaciers of the Flade Isblink  
 Ice Cap. Pink/yellow/blue dashed rectangles depict regions 1/2/3, respectively, with depth exceeding  
 725 100 m. The blue contour lines show the bottom depth.

**Figure 4:** Vertical distribution of temperature (red) and salinity (green) profiles over the Wandel Sea  
 shelf ( $\geq 100$  m depth; solid curves) from April and May 2015, over the continental slope (stations 171-  
 173; dashed curves) from June and July 2015 from the Norwegian FRAM 2014-15 ice drift (see Figure  
 3b for station position) and on the Wandel Sea upper continental slope (ARKXXIII/2 268; dotted  
 730 curves) from RV Polarstern on 2 August 2008 [*Kattner, 2009*]. The blue dashed curve is the *in situ*  
 temperature of freezing computed using the mean SN salinity profile (not shown). The yellow shading  
 highlights sub-surface halocline. The blue shading highlights Atlantic-modified Halocline conditioned  
 by the PcW outflow from the Arctic Ocean which comprises the overlying Halostad (gray shading). The  
 peach shading highlights the AW outflow from the Arctic Ocean, underlying the Atlantic-modified  
 735 Polar Water (PrW). The vertical dashed line depicts salinity of 33 that separates the PcW and AW in the  
 western Beaufort Sea [*von Appen and Pickart, 2012*].

**Figure 5:** *In situ* temperature and salinity curves for the CTD stations >100 m depth with  $\sigma_0$  isopycnals  
 presented (dashed grey lines;  $\text{kg m}^{-3}$ ). (a) CTD profiles from Region 2 and 3 that are grouped into  
 Cluster I “Open Water”. (b) CTD profiles from Region 1 that are grouped into Clusters II–V. The



740 halocline layer of the water column is enlarged in Figure 6a where Clusters II-V are distinguished. In  
(a) and (b) we also present an approximation of thermohaline properties for the downstream Atlantic-  
modified PrW over the NEW continental slope (dashed red line; adopted from *Falck*, 2001) and the  
profile from Station 172 over the Wandel Sea continental slope (thin black dashed line. The surface  
freezing temperature is also presented (dashed blue line). An approximation of the meltwater mixing  
745 line from interaction with the glacial tongue is derived from Cluster V (thick black dashed line). The  
panels are shaded according to the corresponding water masses; gray represents the Halostad, while  
green and pink represent the halocline and define the salinity used for clustering.

**Figure 6:** (a) In situ temperature and salinity curves for the CTD profiles grouped into Clusters II–V.  
The mean *TS* characteristics  $\pm 1$  standard deviation (white barred dots) are presented at isopycnal  
750 intervals of  $0.1 \text{ kg m}^{-3}$ . All other designations are similar to those in Figure 5. (b) Temperature and  
salinity curves below the glacier depth for the CTD profiles grouped into Cluster V.

**Figure 7:** Spatial distribution of the *TS* clusters derived from the *TS* analysis. Arrows depict deep water  
pathways.

**Figure 8:** Vertical distribution of temperature ( $^{\circ}\text{C}$ , red), salinity (green) and turbidity (NTU, black) at  
755 station SN15-13 (Cluster V; solid lines) in front of the tidewater glacier. The CDOM fluorescence (ppb)  
from the moored IPT WETLabs Optical sensor shown for 21 April (dashed violet line) and the 21 April  
– 11 May mean (solid violet line) for the same location. An ambient profile from SN15-09 (Cluster II;  
dotted lines) is presented for comparison. The black dotted line at  $\sim 90$  m depth indicates the suggested  
depth of the glacier tongue. The glacier tongue is depicted schematically.

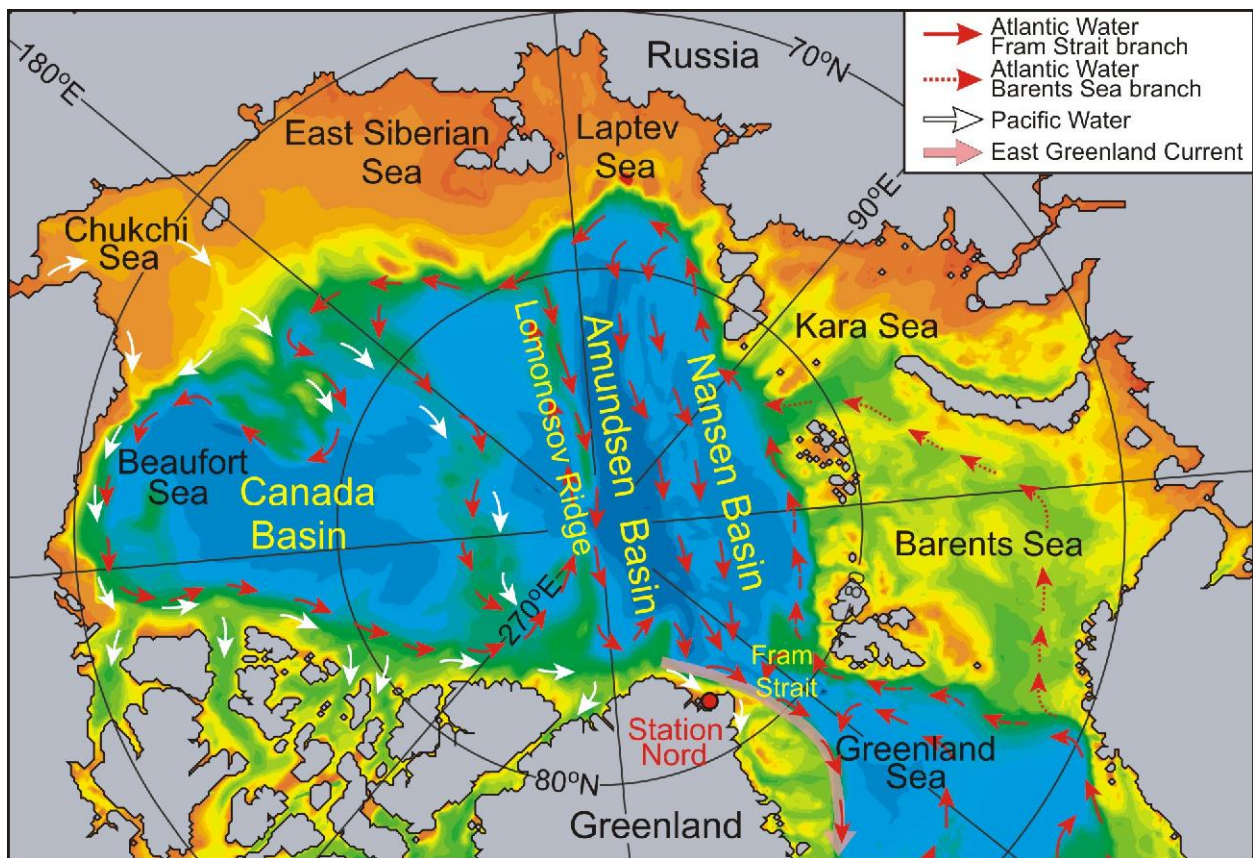


760 **Figure 9: (a)** Schematic showing formation of the intrusive halocline in Clusters III and IV due to  
interleaving between the PcW (blue curve) and PrW (red dotted curve). Gray curve depicts the intrusive  
activity. The black dashed curve is station 172 from the Wandel Sea continental slope. The dashed red  
curve is approximation of the downstream PrW and AW properties at the Greenland continental slope,  
the NEW area adopted from **(b)**. The solid dark/light blue curves are approximations of the PcW and  
765 upper AW from Clusters I/II. The dashed blue curve is approximation of the AW properties over the  
Greenland shelf in the NEW area adopted from **(b)**. The gray dashed lines are  $\sigma_0$  isopycnals in  $\text{kg m}^{-3}$ .  
**(b)** Temperature and salinity curves for the CTD stations taken in July-August 1993 between  $76.5^\circ\text{N}$   
and  $81^\circ\text{N}$  and west of  $5^\circ\text{W}$  over the NEW area after *Falck* [2001]. Blue circles depict stations from the  
polynya (shelf) area. Red rectangular depict stations from the Greenland continental slope and Belgica  
770 Trough. **(a, b)** Blue shading highlights the approximate properties of the Wandel Sea shelf halocline.  
The dashed dark blue line is surface freezing temperature.

**Figure 10: (a)** Temperature ( $^\circ\text{C}$ ) and **(b)** salinity distributions across the Beaufort Sea continental slope  
compiled based on 201 ArcticNet CTD profiles occupied between the  $225^\circ\text{E}$  and  $226^\circ\text{E}$  meridians from  
June to October 2002-2011 (adopted from *Dmitrenko et al.*, 2016). **(c)** In situ mean temperature and  
775 salinity curves for the cross-slope Beaufort Sea section (red) and the Wandel Sea shelf CTD profiles  
from the “basic” Cluster II (black). Shading depicts  $\pm 1$  standard deviation. The red and black dotted  
rectangles indicate thermohaline properties of the Halostad over the Beaufort Sea continental slope and  
Wandel Sea shelf, respectively. The dashed blue line is surface freezing temperature. The gray dashed  
lines are  $\sigma_0$  isopycnals in  $\text{kg m}^{-3}$ .



780 **Figures**



785

**Figure 1:** Schematic circulation of the Atlantic Water (AW, red arrows) and Pacific Water (PcW, white arrows) in the Arctic Ocean and adjoining Greenland Sea following *Rudels et al.* [1994], *Jones* [2001], *Rudels* [2012], and *Woodgate* [2013]. The dashed and dotted red arrows correspond to the Fram Strait and Barents Sea branches of the AW inflow, respectively. The pink arrow indicates the East Greenland Current. The red dot depicts the position of Station Nord in Northeast Greenland.

790



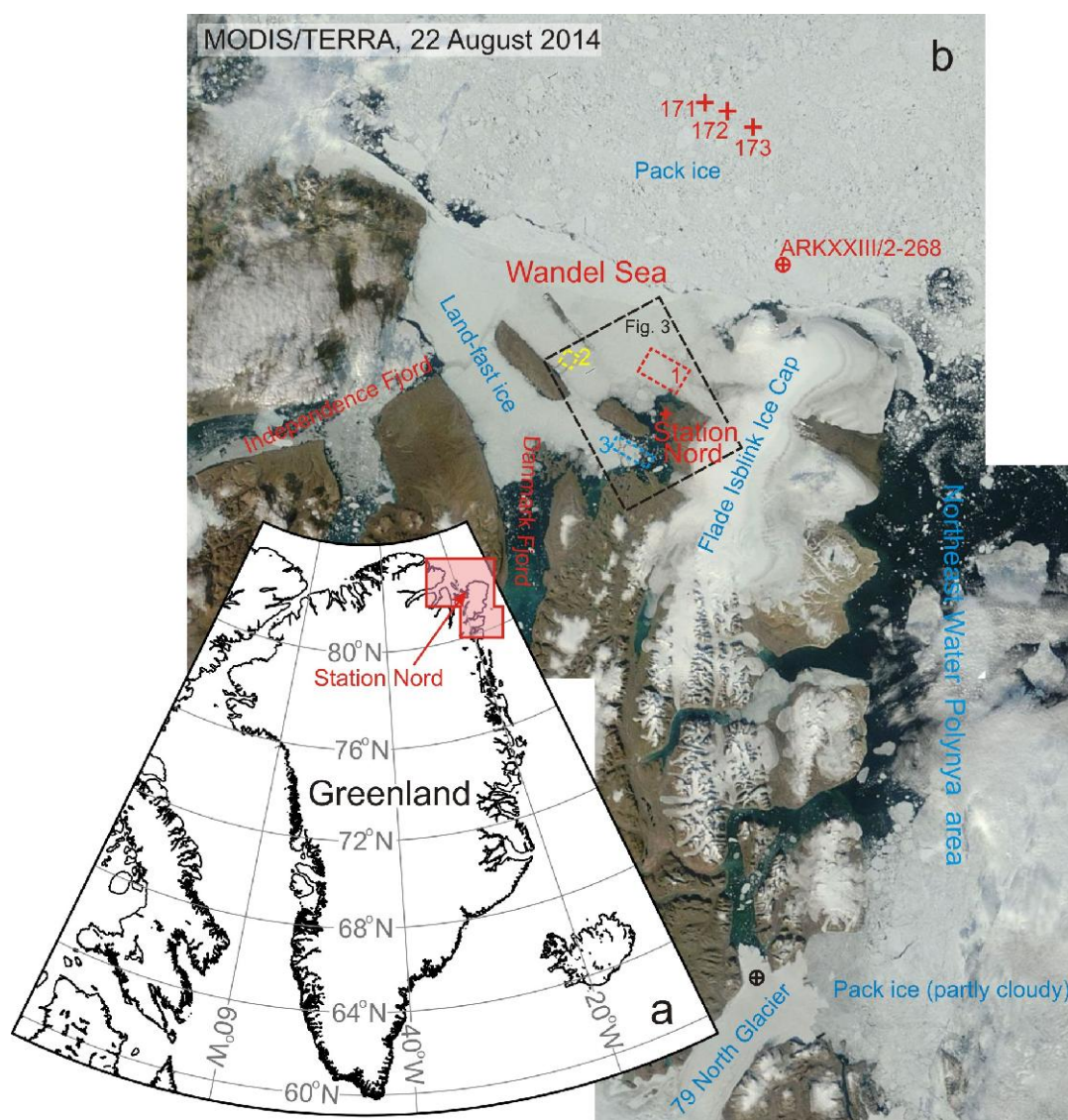


**Figure 2:** (a) Station Nord (SN) on the Greenland map. The pink shading highlights the Wandel Sea region with adjoining fjord system, Flade Isblink Ice Cap (FIIC), the Northeast Water Polynya (NEW) area and the 79 North Glacier outlet enlarged in panel (b). (b) The MODIS/TERRA satellite image from 22 August 2014 taken over the SN/FIIC/NEW area. Red and black circled crosses indicate the CTD stations occupied over the Wandel Sea outer-shelf during the ARKXXIII/2 expedition in August 2008 and in a rift in the 79 North Glacier in August 2009. Red crosses depict the CTD stations occupied in June-July 2015 over the Wandel Sea continental slope (> 1000 m depth) during the Norwegian FRAM 2014-15 sea ice drift. The dashed blue rectangle indicates the 2014 study area shown in Figure 3. Red/yellow/blue dashed rectangles depict regions 1/2/3, respectively, with depth exceeding 100 m.

795

800

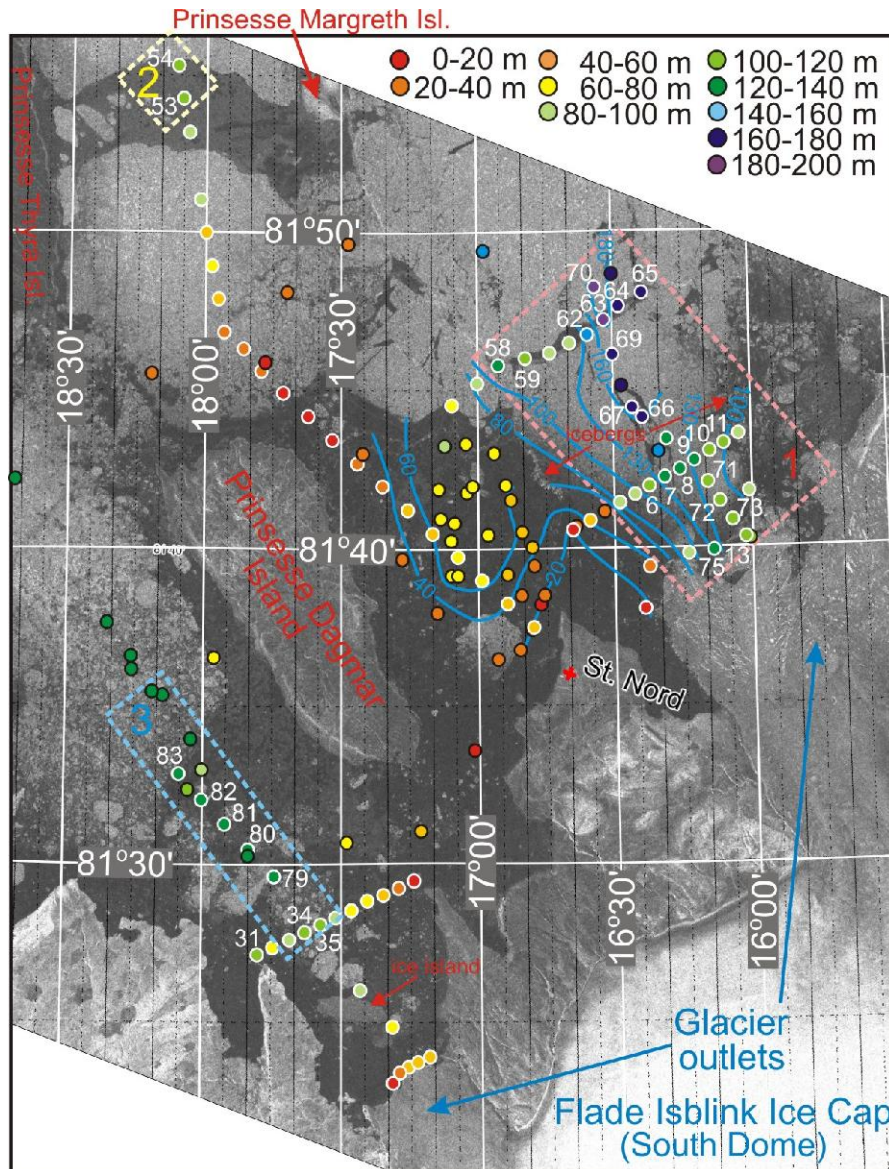


**Figure 3:** The Sentinel-1 C-SAR image from 2 February 2015 with the CTD stations overlaid. The dark areas along the coast are associated with first year landfast ice (< 1.8 m thick). The lighter areas indicate the multi-year landfast ice (~2 m to > 4 m thick). White and black circles identify stations with CTD (April-May 2015) and depth (May 2006, adopted from *Nørgaard-Pedersen et al.* [2008] and April 2015) measurements, respectively, with depths shown by color. CTD stations > 100 m deep are identified by their station numbers. Blue arrows indicate the northern outlet glaciers of the Flade Isblink Ice Cap. Pink/yellow/blue dashed rectangles depict regions 1/2/3, respectively, with depth exceeding 100 m. The blue contour lines show the bottom depth.

805

810



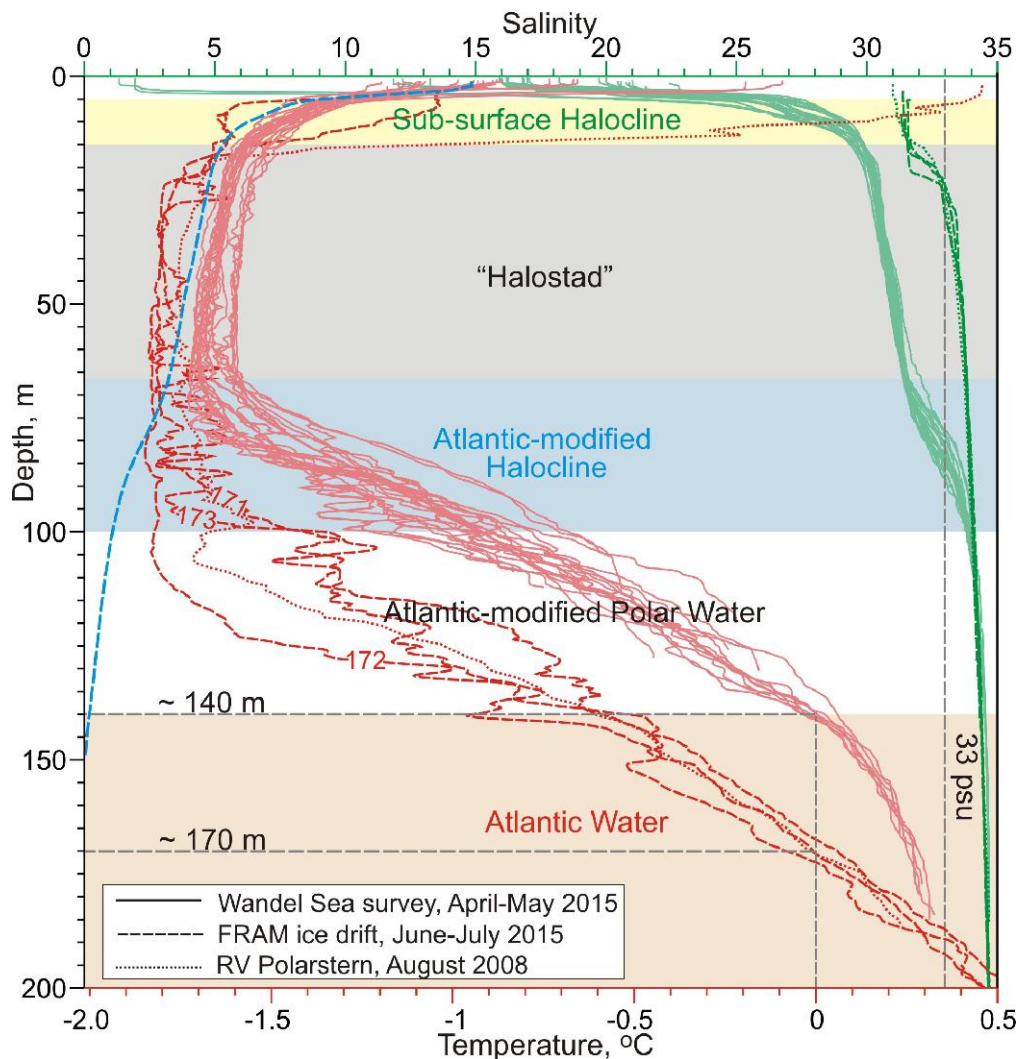


**Figure 4:** Vertical distribution of temperature (red) and salinity (green) profiles over the Wandel Sea shelf ( $\geq 100$  m depth; solid curves) from April and May 2015, over the continental slope (stations 171-173; dashed curves) from June and July 2015 from the Norwegian FRAM 2014-15 ice drift (see Figure 2b for station position) and on the Wandel Sea upper continental slope (ARKXXIII/2 268; dotted curves) from RV Polarstern on 2 August 2008 [Kattner, 2009]. The blue dashed curve is the *in situ* temperature of freezing computed using the mean SN salinity profile (not shown). The yellow shading highlights sub-surface halocline. The blue shading highlights Atlantic-modified Halocline conditioned by the PcW outflow from the Arctic Ocean which comprises the overlying Halostad (gray shading). The peach shading highlights the AW outflow from the Arctic Ocean, underlying the Atlantic-modified Polar water (PrW). The vertical dashed line depicts salinity of 33 that separates the PcW and AW in the western Beaufort Sea [von Appen and Pickart, 2012].



825

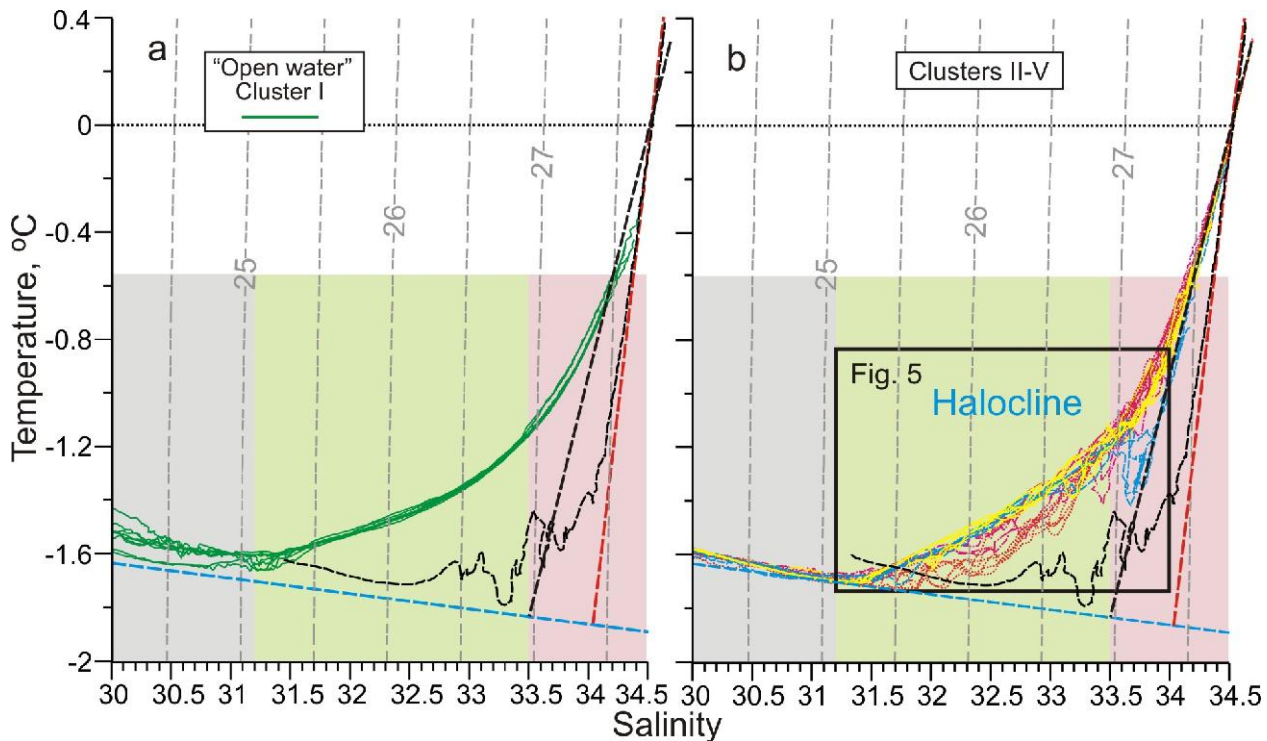


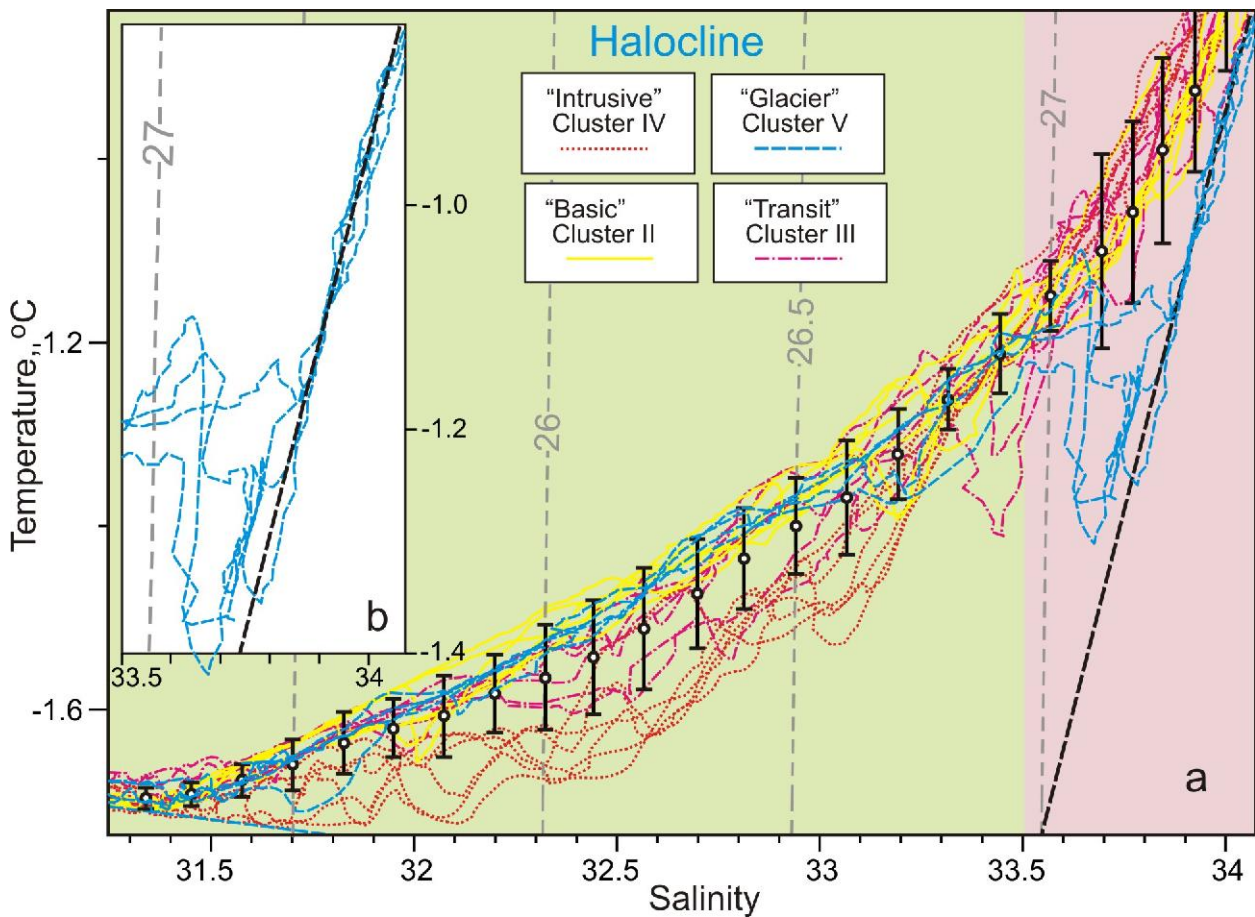
**Figure 5:** *In situ* temperature and salinity curves for the CTD stations >100 m depth with  $\sigma_0$  isopycnals presented (dashed grey lines;  $\text{kg m}^{-3}$ ). (a) CTD profiles from Region 2 and 3 that are grouped into Cluster I “Open Water”. (b) CTD profiles from Region 1 that are grouped into Clusters II–V. The halocline layer of the water column is enlarged in Figure 5a where Clusters II–V are distinguished. We also present an approximation of thermohaline properties for the downstream Atlantic-modified PrW over the NEW continental slope (dashed red line; adopted from Falck, 2001) and the profile from Station 172 over the Wandel Sea continental slope (thin black dashed line). The surface freezing temperature is also presented (dashed blue line). An approximation of the meltwater mixing line from interaction with the glacial tongue is derived from Cluster V (thick black dashed line). The panels are shaded according to the corresponding water masses; gray represents the Halostad, while green and pink represent the halocline and define the salinity used for clustering.

830

835



840



845

**Figure 6:** (a) In situ temperature and salinity curves for the CTD profiles grouped into Clusters II–V. The mean TS characteristics  $\pm 1$  standard deviation (white barred dots) are presented at isopycnal intervals of  $0.1 \text{ kg m}^{-3}$ . All other designations are similar to those in Figure 5. (b) Temperature and salinity curves below the glacier depth for the CTD profiles grouped into Cluster V.

850

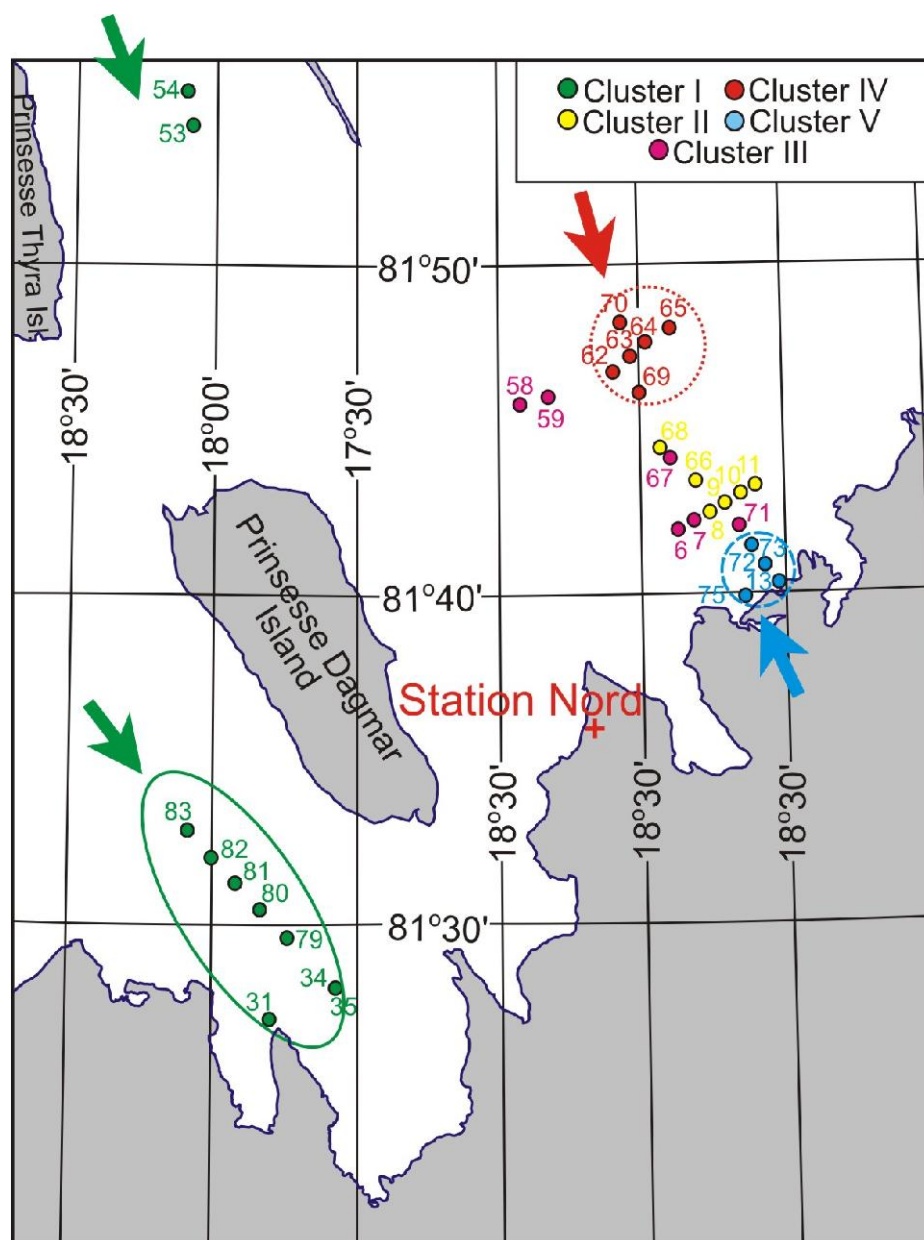


**Figure 7:** Spatial distribution of the *TS* clusters derived from the *TS* analysis. Arrows depict deep water pathways.

855



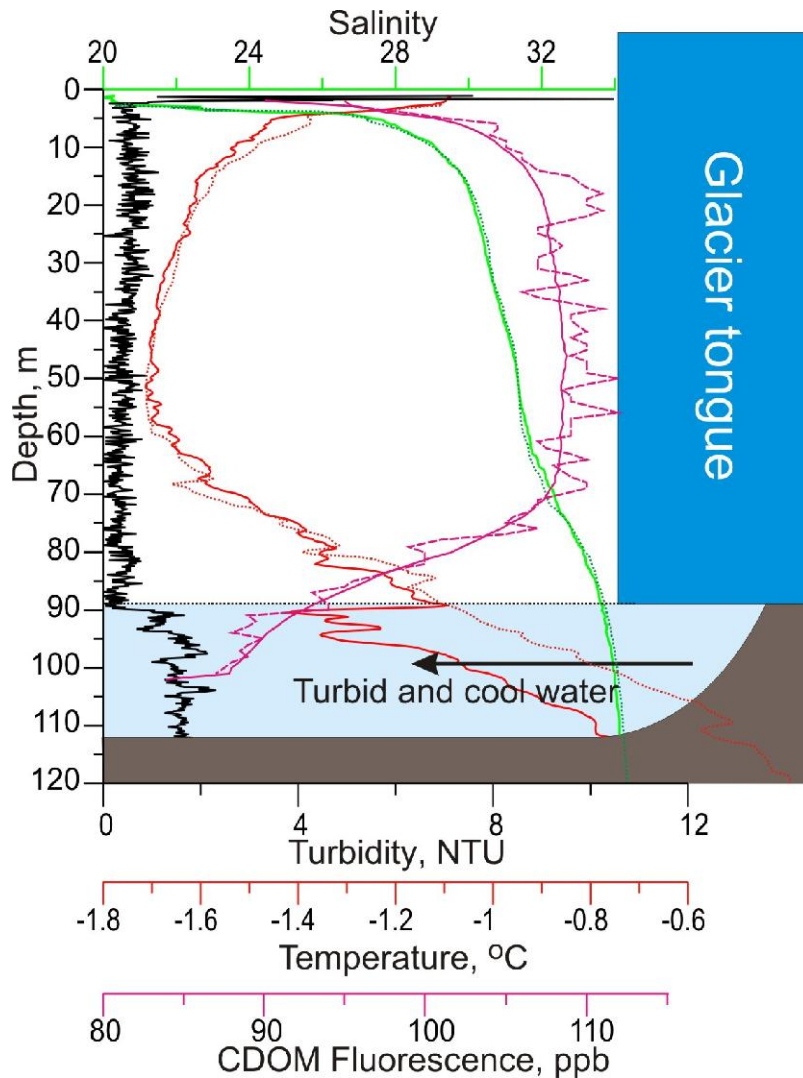
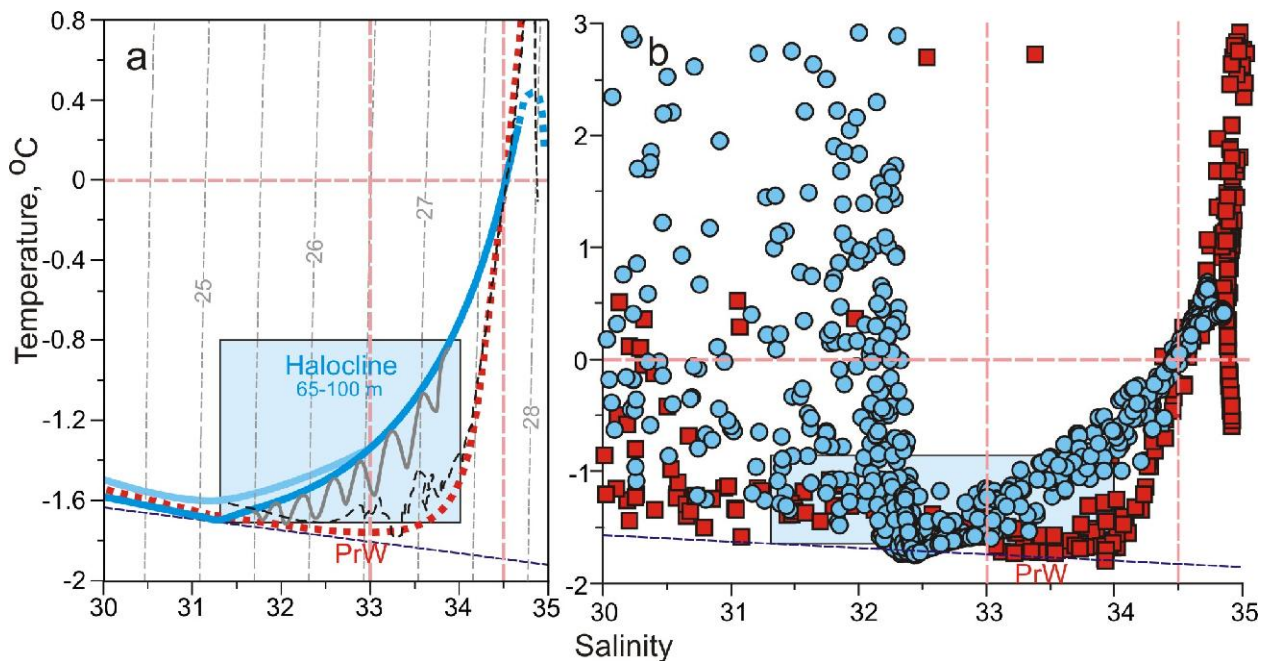


**Figure 8:** Vertical distribution of temperature ( $^{\circ}\text{C}$ , red), salinity (green) and turbidity (NTU, black) at station SN15-13 (Cluster V; solid lines) in front of the tidewater glacier. The CDOM fluorescence (ppb) from the moored IPT WETLabs Optical sensor shown for 21 April (dashed violet line) and the 21 April – 11 May mean (solid violet line) for the same location. An ambient profile from SN15-09 (Cluster II; dotted lines) is presented for comparison. The black dotted line at  $\sim 90$  m depth indicates the suggested depth of the glacier tongue. The glacier tongue is depicted schematically.

860



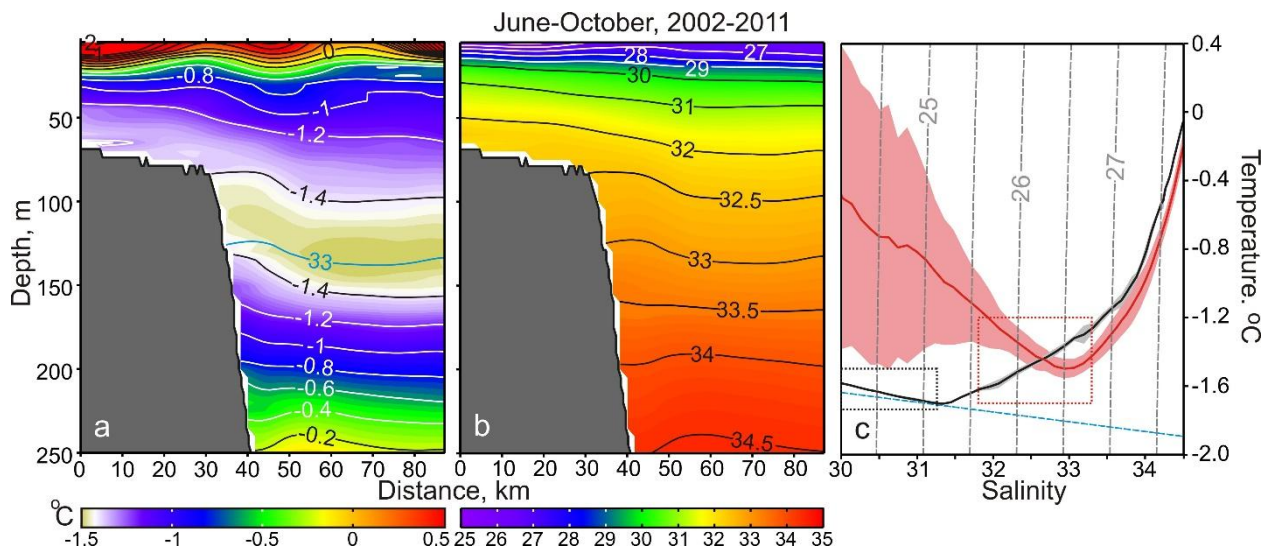
865



870 **Figure 9:** (a) Schematic showing formation of the intrusive halocline in clusters III and IV due to interleaving between the PcW (blue curve) and PrW (red dotted curve). Gray curve depicts the intrusive activity. The black dashed curve is station 172 from the Wandel Sea continental slope. The dashed red curve is approximation of the downstream PrW and AW properties at the Greenland continental slope, the NEW area adopted from (b). The solid dark/light blue curves are approximations of the PcW and upper AW from Clusters I/II. The dashed blue curve is approximation of the AW properties over the Greenland shelf in the NEW area adopted from (b). The gray dashed lines are  $\sigma_0$  isopycnals in  $\text{kg m}^{-3}$ .  
 875 (b) Temperature and salinity curves for the CTD stations taken in July-August 1993 between  $76.5^\circ\text{N}$  and  $81^\circ\text{N}$  and west of  $5^\circ\text{W}$  over the NEW area after Falck [2001]. Blue circles depict stations from the polynya (shelf) area. Red rectangular depict stations from the Greenland continental slope and Belgica Trough. (a, b) Blue shading highlights the approximate properties of the Wandel Sea shelf halocline. The dashed dark blue line is surface freezing temperature.  
 880



885



890 **Figure 10:** (a) Temperature ( $^{\circ}\text{C}$ ) and (b) salinity distributions across the Beaufort Sea continental slope  
compiled based on 201 ArcticNet CTD profiles occupied between the  $225^{\circ}\text{E}$  and  $226^{\circ}\text{E}$  meridians from  
June to October 2002-2011 (adopted from *Dmitrenko et al.*, 2016). (c) In situ mean temperature and  
895 salinity curves for the cross-slope Beaufort Sea section (red) and the Wandel Sea shelf CTD profiles  
from the “basic” Cluster II (black). Shading depicts  $\pm 1$  standard deviation. The red and black dotted  
rectangles indicate thermohaline properties of the Halostad over the Beaufort Sea continental slope and  
Wandel Sea shelf, respectively. The dashed blue line is surface freezing temperature. The gray dashed  
lines are  $\sigma_0$  isopycnals in  $\text{kg m}^{-3}$ .